J. Nonlinear Var. Anal. 9 (2025), No. 6, pp. 833-862
Available online at http://jnva.biemdas.com
https://doi.org/10.23952/jnva.9.2025.6.02

LDG METHOD WITH THE FAST TIME TECHNIQUE FOR THE TWO-DIMENSIONAL FRACTIONAL MOBILE/IMMOBILE CONVECTION-DIFFUSION MODEL

NIAN WANG[1], JINFENG WANG[2], HONG LI[1], FAWANG LIU[3,4], YANG LIU[1,*]

[1]*School of Mathematical Sciences, Inner Mongolia University, Hohhot 010021, China*
[2]*School of Statistics and Mathematics,*
Inner Mongolia University of Finance and Economics, Hohhot 010070, China
[3]*School of Mathematical Sciences,*
Queensland University of Technology, GPO Box 2434, Brisbane, Qld. 4001, Australia
[4]*School of Mathematical and Statistics, Fuzhou University, Fuzhou, 350108, China*

Abstract. In this paper a fast algorithm is presented for numerically solving a two-dimensional fractional mobile/immobile convection-diffusion model, where the second-order time scheme of the integer derivative and the $\mathscr{F}L2\text{-}1_\sigma$ formula of the time Caputo fractional derivative are used in the time direction, and the local discontinuous Galerkin (LDG) method is developed to approximate the space direction. The stability of the fully discrete LDG scheme is proven, and the a priori error result with $O(\Delta t^2 + h^{k+1} + \varepsilon)$ is derived, where ε is the tolerance error. Finally, some numerical results with $Q^k (k = 0, 1, 2)$ elements are given to verify our theoretical results.

Keywords. A priori error result; $\mathscr{F}L2\text{-}1_\sigma$ formula; stability; LDG method; two-dimensional fractional mobile/immobile convection-diffusion model.

1. Introduction

In this paper, we consider the two-dimensional fractional mobile/immobile convection-diffusion model

$$u_t(x,y,t) + {}_0^C D_t^\alpha u(x,y,t) + \gamma \cdot \nabla u(x,y,t) - \Delta u(x,y,t) = f(x,y,t), \quad (x,y,t) \in \Omega \times (0,T], \quad (1.1)$$

with the periodic boundary condition and the initial condition

$$u(x,y,0) = u_0(x,y), \quad (x,y) \in \overline{\Omega}, \quad (1.2)$$

where $\Omega \subset \mathbb{R}^2$, $0 < T < \infty$, $\gamma = (\gamma_1, \gamma_2)^T$, with γ_1, γ_2 being given positive constants, the smooth function $f(x,y,t)$ is the source term, and the ${}_0^C D_t^\alpha u$ is the Caputo time fractional derivative with $\alpha \in (0,1)$, which is given by

$${}_0^C D_t^\alpha u = \frac{1}{\Gamma(1-\alpha)} \int_0^t \frac{\partial u(s)}{\partial s} \frac{ds}{(t-s)^\alpha},$$

*Corresponding author.
E-mail address: mathliuyang@imu.edu.cn (Y. Liu).
Received 19 November 2023; Accepted 12 August 2024; Published online 10 August 2025.

Among fractional partial differential equations, the fractional mobile/immobile convection-diffusion model is a very important mathematical model, which can describe numerous physical phenomena such as solute migration in fractured porous media. Therefore, more and more researchers paid attention to numerical methods for solving the model. Schumer et al. [1] developed the fractional mobile/immobile model for the total concentration. In [2], Zhang et al. proposed an implicit Euler numerical method for the fractional mobile/immobile advection-dispersion model with time variable. In [3], Liu et al. presented the fully discrete characteristic finite element scheme for the model, where the characteristic technique was used to handle the domination of advection. In [4], Yu et al. studied the numerical identification of fractional parameters in the fractional mobile/immobile advection-diffusion model. In [5], Wang et al. studied the mixed finite element scheme for a nonlinear convection-diffusion equation with time fractional derivative. In [6], Chen et al. proposed a fully discrete two-grid modified method of characteristics (MMOC) scheme for a two-dimensional nonlinear variable order time fractional advection-diffusion equation. In [7], based on a weighted and shifted Grünwald-Letnikov difference (WSGD) Legendre spectral method, Zhang et al. numerically solved the two-dimensional nonlinear time fractional mobile/immobile advection-diffusion equation. Because of the existence of fractional orders and convection terms, the analytical solution of the model is difficult to obtain. Therefore, finding a feasible and effective numerical algorithm is very important.

As far as we know, the local discontinuous Galerkin (LDG) method proposed by Cockburn and Shu in [8] can effectively solve fractional order partial differential equations and has gradually become the current research focus. In [9], Liu et al. proposed the LDG method combined with WSGD approximation and discussed a Caputo-type time-fractional diffusion equation. In [10], Li et al. numerically studied three typical Caputo-type partial differential equations by using the finite difference method and the local discontinuous Galerkin finite element analysis. In [11], based on some second-order θ approximation formulas in time, Zhang et al. gave the LDG numerical scheme of the two-dimensional nonlinear fractional diffusion equation. In [12], Niu et al. solved the one-dimensional fractional mobile/immobile convection-diffusion equation by using the LDG method combined with the generalized second-order backward difference formula with a shifted parameter θ (BDF2-θ). For more results on LDG solving fractional order model, we refer to [13–23].

In [24], Alikhanov constructed $L2\text{-}1_\sigma$ formula with approximate order $O(\Delta t^{3-\alpha})$, and studied some basic properties of the formula. On this basis, some difference schemes of time-fractional diffusion equations with variable coefficients were considered, and their stability and convergence were proved. According to the above work, Sun et al. [25] further developed some properties of the $L2\text{-}1_\sigma$ formula and the second-order time approximation scheme, and proposed some difference schemes for one-dimensional and two-dimensional time fractional wave equations. In [26], Huang et al. solved a time-fractional reaction diffusion with discontinuous diffusion coefficient by using the $L2\text{-}1_\sigma$ formula on the graded meshes and the LDG method in space. In [27], Wang et al. used the nonuniform $L1$ formula and the nonuniform $L2\text{-}1_\sigma$ formula combined with the LDG method to obtain a numerical algorithm for the time-fractional Allen-Cahn equation with a weak singularity solution.

In the process of computing fractional derivative by numerical techniques, the value of some time layer needs to use the value of all previous time layers, leading to a large amount of computation. Therefore, it is very meaningful to study effective and fast algorithms. Recently, Jiang et al. [28] studied a fast algorithm for approximating the Caputo fractional derivative based on the $L1$ formula and sum-of-exponentials (SOE) approximation. In this algorithm, the computation of each layer is reduced by exponential summation and approximate kernel $t^{-\alpha}$ without reducing the accuracy of the $L1$ formula. In [29], Yan et al. developed the $\mathscr{F}L2\text{-}1_\sigma$ formula by using the $L2\text{-}1_\sigma$ formula and SOE approximation, solved the fractional diffusion equation effectively, and increased the calculation speed. In [30], Liang et al. proposed a fast high-order difference algorithm for time fractional telegraph equation based on $\mathscr{F}L2\text{-}1_\sigma$ formula of Caputo fractional derivative. For more details on the SOE approximation, we refer to [31–34].

In this paper, we combine the second-order time approximation scheme with the $\mathscr{F}L2\text{-}1_\sigma$ formula to approximate the time-fractional derivative and develop the LDG method in spaces and to solve two-dimensional fractional mobile/immobile convection-diffusion model (1.1). The main contributions of this paper are as follows.

- A fully discrete LDG scheme based on the second-order time approximation scheme and $\mathscr{F}L2\text{-}1_\sigma$ formula is given;
- The stability of the LDG scheme is proven. Then, the a priori error estimates with second-order temporal convergence rate and high-order spatial convergence rate are obtained;
- Numerical tests based on $Q^k(k=0,1,2)$ elements in space to verify the theoretical results, and the convergence accuracy and computation speed of $\mathscr{F}L2\text{-}1_\sigma$ scheme and $L2\text{-}1_\sigma$ scheme are compared.

The organization of this paper is as follows. In Section 2, a fully discrete LDG numerical scheme is proposed. The stability of the scheme is proved in Section 3. In Section 4, the error estimate of the fully discrete scheme is confirmed. In Section 5, the results of the theoretical analysis are verified by some numerical results. In Section 6, the last section, some conclusions are given.

2. Fully Discrete Scheme

Symbols commonly used in the LDG method are introduced. To divide space domain $\bar{\Omega}_x \times \bar{\Omega}_y = [L_a, L_b] \times [L_c, L_d]$, we define the mesh $I_{ij} = I_i \otimes J_j$, where $I_i = [x_{i-\frac{1}{2}}, x_{i+\frac{1}{2}}]$ and $J_j = [y_{j-\frac{1}{2}}, y_{j+\frac{1}{2}}]$, for $i = 1, \cdots, N_x$ and $j = 1, \cdots, N_y$. The cell lengths are denoted by $\Delta x_i = x_{i+\frac{1}{2}} - x_{i-\frac{1}{2}}$ and $\Delta y_j = y_{j+\frac{1}{2}} - y_{j-\frac{1}{2}}$ with $h = \max_{i,j}\{\Delta x_i, \Delta y_j\}$. The jump value of u on each element boundary is defined as $[\![u(x_{i+\frac{1}{2}}, y)]\!] = u(x^+_{i+\frac{1}{2}}, y) - u(x^-_{i+\frac{1}{2}}, y)$ and $[\![u(x, y_{j+\frac{1}{2}})]\!] = u(x, y^+_{j+\frac{1}{2}}) - u(x, y^-_{j+\frac{1}{2}})$.

First, we split problem (1.1) to the following coupled system by introducing two auxiliary variables $q = u_x$ and $p = u_y$,

$$\begin{cases} q = u_x, \\ p = u_y, \\ u_t + {}_0^C D_t^\alpha u + \gamma_1 u_x + \gamma_2 u_y - q_x - p_y = f(x,y,t). \end{cases}$$

To solve our problem, we insert node $t_n = n\Delta t$ in the time interval $[0,T]$, where $0 = t_0 < t_1 < \cdots\cdots < t_M = T$, $\Delta t = T/M$ with some integer $M > 0$. For simplicity, we define $\chi^n = \chi(t_n)$ for a smooth function χ on $[0,T]$. Then, we provide two lemmas about and time integer derivative.

Lemma 2.1. *(See [25]) Let $\sigma = 1-\frac{\alpha}{2}$. At time $t_{n+\sigma}$, the following formula holds,*

$$v_t(t_{n+\sigma}) = \begin{cases} \dfrac{(2\sigma+1)v^{n+1}-4\sigma v^n+(2\sigma-1)v^{n-1}}{2\Delta t}+O(\Delta t^2), \\ \dfrac{v^1-v^0}{\Delta t}+O(\Delta t), \end{cases}$$
$$\triangleq \partial_{\Delta t}^{\sigma} v^{n+1} + \begin{cases} O(\Delta t^2), n\geq 1, \\ O(\Delta t), n=0, \end{cases}$$

Lemma 2.2. *At time $t_{n+\sigma}$, the following important relationship holds*

$$v(t_{n+\sigma}) = \sigma v^{n+1}+(1-\sigma)v^n+O(\Delta t^2) \triangleq v^{n+\sigma}+O(\Delta t^2).$$

Proof. It can be proved by Taylor's formula and simple calculation. □

To provide $\mathscr{F}L2\text{-}1_{\sigma}$ formula, we first review $L2\text{-}1_{\sigma}$ formula.

Lemma 2.3. *(See [24]) Let $v(t)\in C^3[0,T]$. Then, the following time approximation formula at time $t_{n+\sigma}$ holds, for $\alpha\in(0,1)$,*

$${}_0^C D_t^{\alpha} v(t_{n+\sigma}) = \frac{\Delta t^{-\alpha}}{\Gamma(2-\alpha)} \sum_{l=0}^{n} r_{n-l}^{(n+1)}(v^{l+1}-v^l)+O(\Delta t^{3-\alpha}),$$
$$\triangleq D_t^{\alpha}[v^{n+\sigma}]+O(\Delta t^{3-\alpha}),$$

where, for $n\geq 1$,

$$r_s^{(n+1)} = \begin{cases} a_0^{(\alpha,\sigma)}+b_1^{(\alpha,\sigma)}, & s=0, \\ a_s^{(\alpha,\sigma)}+b_{s+1}^{(\alpha,\sigma)}-b_s^{(\alpha,\sigma)}, & 1\leq s\leq n-1, \\ a_n^{(\alpha,\sigma)}+b_n^{(\alpha,\sigma)}, & s=n, \end{cases}$$

for $n=0$, $r_0^{(\alpha,\sigma)} = a_0^{(\alpha,\sigma)}$ and

$$a_0^{(\alpha,\sigma)} = \sigma^{1-\alpha}, a_m^{(\alpha,\sigma)} = (m+\sigma)^{1-\alpha}-(m-1+\sigma)^{1-\alpha}, m\geq 1,$$
$$b_m^{(\alpha,\sigma)} = \frac{1}{2-\alpha}[(m+\sigma)^{2-\alpha}-(m-1+\sigma)^{2-\alpha}]+\frac{1}{2}[(m+\sigma)^{1-\alpha}-(m-1+\sigma)^{1-\alpha}], m\geq 1.$$

Next, we review the core idea of SOE, which is to effectively approximate the kernel $t^{-\alpha}$ by summing exponentially.

Lemma 2.4. *(See [28, 29]) For the given $\alpha\in(0,1)$, tolerance error ε, cut-off time step size δ and final time T, there exist positive real numbers s_m and w_m $(m=1,\cdots,N_{exp})$ satisfy*

$$\left| t^{-\alpha} - \sum_{m=1}^{N_{exp}} w_m e^{-s_m t} \right| \leq \varepsilon, \quad t\in[\delta,T],$$

where

$$N_{exp} = O\left(\log\frac{1}{\varepsilon}\left(\log\log\frac{1}{\varepsilon}+\log\frac{T}{\delta}\right)+\log\frac{1}{\delta}\left(\log\log\frac{1}{\varepsilon}+\log\frac{1}{\delta}\right)\right).$$

Then, we simply introduce the $\mathscr{F}L2\text{-}1_{\sigma}$ formula, as detailed in [29]. The Caputo fractional derivative ${}_0^C D_t^{\alpha} v(t_{n+\sigma})$ is divided into the historical part and the local part. The kernel $t^{-\alpha}$ is approximated by SOE in the history part, and $v'(s)$ is treated by linear interpolation in the local part, to arrive at

$$\begin{aligned} {}_0^C D_t^\alpha v(t_{n+\sigma}) &= \frac{1}{\Gamma(1-\alpha)} \int_0^{t_{n+\sigma}} \frac{v'(s)}{(t_{n+\sigma}-s)^\alpha} ds \\ &= \frac{1}{\Gamma(1-\alpha)} \left(\int_0^{t_n} \frac{v'(s)}{(t_{n+\sigma}-s)^\alpha} ds + \int_{t_n}^{t_{n+\sigma}} \frac{v'(s)}{(t_{n+\sigma}-s)^\alpha} ds \right) \\ &\approx \frac{1}{\Gamma(1-\alpha)} \left(\int_0^{t_n} v'(s) \sum_{m=1}^{N_{exp}} w_m e^{-s_m(t_{n+\sigma}-s)} ds + \frac{v^{n+1}-v^n}{\Delta t} \int_{t_n}^{t_{n+\sigma}} \frac{ds}{(t_{n+\sigma}-s)^\alpha} \right) \\ &\approx \sum_{m=1}^{N_{exp}} \hat{w}_m V_m^n + \lambda a_0 (v^{n+1}-v^n) = {}^{\mathscr{F}}D_t^\alpha v^{n+\sigma}, \end{aligned}$$

where $\lambda = \frac{\Delta t^{-\alpha}}{\Gamma(2-\alpha)}, \hat{w}_m = \frac{1}{\Gamma(1-\alpha)} w_m$, $a_0 = \sigma^{1-\alpha}$, and the iteration for the history part of the integral is

$$V_m^n = e^{-s_m \Delta t} V_m^{n-1} + A_m (v^n - v^{n-1}) + B_m (v^{n+1} - v^n)$$

with $V_m^0 = 0$ $(m = 1, \cdots, N_{exp})$,

$$A_m = \int_0^1 (\frac{3}{2} - s) e^{-s_m \Delta t (\sigma+1-s)} ds, \quad B_m = \int_0^1 (s - \frac{1}{2}) e^{-s_m \Delta t (\sigma+1-s)} ds.$$

To facilitate the theoretical analysis, we present the following equivalent form of $\mathscr{F}L2\text{-}1_\sigma$ formula

$${}^{\mathscr{F}}D_t^\alpha v^{n+\sigma} = \sum_{l=0}^{n} {}^{\mathscr{F}}g_l^{(n+1)} (v^{l+1} - v^l),$$

where

$${}^{\mathscr{F}}g_l^{(n+1)} = \begin{cases} \sum_{m=1}^{N_{exp}} \hat{w}_m e^{-(n-1)s_m \Delta t} A_m, & l = 0, \\ \sum_{m=1}^{N_{exp}} \hat{w}_m (e^{-(n-l-1)s_m \Delta t} A_m + e^{-(n-l)s_m \Delta t} B_m), & 1 \le l \le n-1, \\ \sum_{m=1}^{N_{exp}} \hat{w}_m B_m + \lambda a_0, & l = n. \end{cases}$$

Further, based on the above $\mathscr{F}L2\text{-}1_\sigma$ formula, we have the following lemma.

Lemma 2.5. *(See [29]) Suppose the function $v(t) \in C^3[0,T]$. For $\alpha \in (0,1)$, it holds*

$${}_0^C D_t^\alpha v(t_{n+\sigma}) = {}^{\mathscr{F}}D_t^\alpha v^{n+\sigma} + O(\Delta t^{3-\alpha} + \varepsilon), \quad n = 0, \cdots, M-1.$$

According to the above formulas, we see that

$$\begin{cases} q^{n+\sigma} - u_x^{n+\sigma} = R_1^{n+\sigma}, \\ p^{n+\sigma} - u_y^{n+\sigma} = R_2^{n+\sigma}, \\ \partial_{\Delta t}^\sigma u^{n+1} + {}^{\mathscr{F}}D_t^\alpha u^{n+\sigma} + \gamma_1 u_x^{n+\sigma} + \gamma_2 u_y^{n+\sigma} - q_x^{n+\sigma} - p_y^{n+\sigma} = f^{n+\sigma} + R_3^{n+\sigma} + R_4^{n+\sigma} + R_5^{n+\sigma}, \end{cases} \tag{2.1}$$

where

$$
\begin{aligned}
R_1^{n+\sigma} =& q^{n+\sigma}-q(t_{n+\sigma})-(u_x^{n+\sigma}-u_x(t_{n+\sigma}))=O(\Delta t^2),\\
R_2^{n+\sigma} =& p^{n+\sigma}-p(t_{n+\sigma})-(u_y^{n+\sigma}-u_y(t_{n+\sigma}))=O(\Delta t^2),\\
R_3^{n+\sigma} =& {}^{\mathscr{F}}D_t^{\alpha}u^{n+\sigma}-{}_0^C D_t^{\alpha}u(t_{n+\sigma})=O(\Delta t^{3-\alpha}+\varepsilon),\\
R_4^{n+\sigma} =& \partial_{\Delta t}^{\sigma}u^{n+1}-u_t(t_{n+\sigma})=\begin{cases}O(\Delta t^2), & n\geq 1,\\ O(\Delta t), & n=0,\end{cases}\\
R_5^{n+\sigma} =& (u_x^{n+\sigma}-u_x(t_{n+\sigma}))+(u_y^{n+\sigma}-u_y(t_{n+\sigma}))-(q_x^{n+\sigma}-q_x(t_{n+\sigma}))\\
&-(p_y^{n+\sigma}-p_y(t_{n+\sigma}))-(f^{n+\sigma}-f(t_{n+\sigma}))=O(\Delta t^2).
\end{aligned}
\tag{2.2}
$$

To further obtain the fully discrete scheme, we define the finite element space V_h^k as follows

$$
V_h^k=\left\{v\in L^2(\Omega): v|_{I_{ij}}\in Q^k(I_{ij}), i=1,\cdots,N_x, j=1,\cdots,N_y\right\},
$$

where $Q^k(I_{ij})=P^k(I_i)\otimes P^k(J_j)$ and $P^k(I_i)$ is a set of local orthogonal polynomials of up to degree k in I_i. The inner product and corresponding L^2-norm on Ω are defined by $(u,v)=\int_\Omega uvdxdy$ and $\|u\|^2=(u,u)$.

Multiplying (2.1) by the test functions w,φ,v, we have the following weak formulation of (2.1)

$$
\begin{aligned}
&\int_\Omega q^{n+\sigma}wdxdy+\sum_{i,j}\int_{I_{i,j}}u^{n+\sigma}w_xdxdy-\int_{\Omega_y}\sum_{i=1}^{N_x}\left[\left(u^{n+\sigma}\left(x_{i+\frac12},y\right)w\left(x_{i+\frac12}^-,y\right)\right)\right.\\
&\left.-\left(u^{n+\sigma}\left(x_{i-\frac12},y\right)w\left(x_{i-\frac12}^+,y\right)\right)\right]dy=\int_\Omega R_1^{n+\sigma}wdxdy,\quad \forall w\in L^2(I_{ij}),
\end{aligned}
\tag{2.3}
$$

$$
\begin{aligned}
&\int_\Omega p^{n+\sigma}\varphi dxdy+\sum_{i,j}\int_{I_{i,j}}u^{n+\sigma}\varphi_ydxdy-\int_{\Omega_x}\sum_{j=1}^{N_y}\left[\left(u^{n+\sigma}\left(x,y_{j+\frac12}\right)\varphi\left(x,y_{j+\frac12}^-\right)\right)\right.\\
&\left.-\left(u^{n+\sigma}\left(x,y_{j-\frac12}\right)\varphi\left(x,y_{j-\frac12}^+\right)\right)\right]dx=\int_\Omega R_2^{n+\sigma}\varphi dxdy,\quad \forall \varphi\in L^2(I_{ij}),
\end{aligned}
\tag{2.4}
$$

and

$$
\begin{aligned}
&\int_\Omega \partial_{\Delta t}^{\sigma}u^{n+1}vdxdy+\int_\Omega {}^{\mathscr{F}}D_t^{\alpha}u^{n+\sigma}vdxdy-\gamma_1\sum_{i,j}\int_{I_{i,j}}u^{n+\sigma}v_xdxdy-\gamma_2\sum_{i,j}\int_{I_{i,j}}u^{n+\sigma}v_ydxdy\\
&+\sum_{i,j}\int_{I_{i,j}}q^{n+\sigma}v_xdxdy+\sum_{i,j}\int_{I_{i,j}}p^{n+\sigma}v_ydxdy+\gamma_1\int_{\Omega_y}\sum_{i=1}^{N_x}\left[\left(u^{n+\sigma}\left(x_{i+\frac12},y\right)v\left(x_{i+\frac12}^-,y\right)\right)\right.\\
&\left.-\left(u^{n+\sigma}\left(x_{i-\frac12},y\right)v\left(x_{i-\frac12}^+,y\right)\right)\right]dy+\gamma_2\int_{\Omega_x}\sum_{j=1}^{N_y}\left[\left(u^{n+\sigma}\left(x,y_{j+\frac12}\right)v\left(x,y_{j+\frac12}^-\right)\right)\right.\\
&\left.-\left(u^{n+\sigma}\left(x,y_{j-\frac12}\right)v\left(x,y_{j-\frac12}^+\right)\right)\right]dx-\int_{\Omega_y}\sum_{i=1}^{N_x}\left[\left(q^{n+\sigma}\left(x_{i+\frac12},y\right)v\left(x_{i+\frac12}^-,y\right)\right)\right.\\
&\left.-\left(q^{n+\sigma}\left(x_{i-\frac12},y\right)v\left(x_{i-\frac12}^+,y\right)\right)\right]dy-\int_{\Omega_x}\sum_{j=1}^{N_y}\left[\left(p^{n+\sigma}\left(x,y_{j+\frac12}\right)v\left(x,y_{j+\frac12}^-\right)\right)\right.\\
&\left.-\left(p^{n+\sigma}\left(x,y_{j-\frac12}\right)v\left(x,y_{j-\frac12}^+\right)\right)\right]dx=\int_\Omega f^{n+\sigma}vdxdy+\int_\Omega R_3^{n+\sigma}vdxdy\\
&+\int_\Omega R_4^{n+\sigma}vdxdy+\int_\Omega R_5^{n+\sigma}vdxdy,\quad \forall v\in L^2(I_{ij}).
\end{aligned}
\tag{2.5}
$$

Let $q_h^{n+1}, p_h^{n+1}, u_h^{n+1} \in V_h^k$ be the approximation of $q^{n+1}, p^{n+1}, u^{n+1}$, respectively. The fully discrete scheme at time $t_{n+\sigma}$ is given as follows

$$\begin{aligned}&\int_\Omega q_h^{n+\sigma} w dxdy + \sum_{i,j}\int_{I_{i,j}} u_h^{n+\sigma} w_x dxdy - \int_{\Omega_y}\sum_{i=1}^{N_x}\Big[\Big(\tilde{u}_h^{n+\sigma}\left(x_{i+\frac{1}{2}},y\right) w\left(x_{i+\frac{1}{2}}^-,y\right)\Big)\\&-\Big(\tilde{u}_h^{n+\sigma}\left(x_{i-\frac{1}{2}},y\right) w\left(x_{i-\frac{1}{2}}^+,y\right)\Big)\Big] dy = 0, \quad \forall w \in V_h^k,\end{aligned} \tag{2.6}$$

$$\begin{aligned}&\int_\Omega p_h^{n+\sigma} \varphi dxdy + \sum_{i,j}\int_{I_{i,j}} u_h^{n+\sigma} \varphi_y dxdy - \int_{\Omega_x}\sum_{j=1}^{N_y}\Big[\Big(\tilde{u}_h^{n+\sigma}\left(x,y_{j+\frac{1}{2}}\right) \varphi\left(x,y_{j+\frac{1}{2}}^-\right)\Big)\\&-\Big(\tilde{u}_h^{n+\sigma}\left(x,y_{j-\frac{1}{2}}\right) \varphi\left(x,y_{j-\frac{1}{2}}^+\right)\Big)\Big] dx = 0, \quad \forall \varphi \in V_h^k,\end{aligned} \tag{2.7}$$

and

$$\begin{aligned}&\int_\Omega \partial_{\Delta t}^\sigma u_h^{n+1} v dxdy + \int_\Omega {}^{\mathscr{F}}D_t^\alpha u_h^{n+\sigma} v dxdy - \gamma_1 \sum_{i,j}\int_{I_{i,j}} u_h^{n+\sigma} v_x dxdy - \gamma_2 \sum_{i,j}\int_{I_{i,j}} u_h^{n+\sigma} v_y dxdy\\&+\sum_{i,j}\int_{I_{i,j}} q_h^{n+\sigma} v_x dxdy + \sum_{i,j}\int_{I_{i,j}} p_h^{n+\sigma} v_y dxdy + \gamma_1\int_{\Omega_y}\sum_{i=1}^{N_x}\Big[\Big(\tilde{u}_h^{n+\sigma}\left(x_{i+\frac{1}{2}},y\right) v\left(x_{i+\frac{1}{2}}^-,y\right)\Big)\\&-\Big(\tilde{u}_h^{n+\sigma}\left(x_{i-\frac{1}{2}},y\right) v\left(x_{i-\frac{1}{2}}^+,y\right)\Big)\Big] dy + \gamma_2\int_{\Omega_x}\sum_{j=1}^{N_y}\Big[\Big(\tilde{u}_h^{n+\sigma}\left(x,y_{j+\frac{1}{2}}\right) v\left(x,y_{j+\frac{1}{2}}^-\right)\Big)\\&-\Big(\tilde{u}_h^{n+\sigma}\left(x,y_{j-\frac{1}{2}}\right) v\left(x,y_{j-\frac{1}{2}}^+\right)\Big)\Big] dx - \int_{\Omega_y}\sum_{i=1}^{N_x}\Big[\Big(\tilde{q}_h^{n+\sigma}\left(x_{i+\frac{1}{2}},y\right) v\left(x_{i+\frac{1}{2}}^-,y\right)\Big)\\&-\Big(\tilde{q}_h^{n+\sigma}\left(x_{i-\frac{1}{2}},y\right) v\left(x_{i-\frac{1}{2}}^+,y\right)\Big)\Big] dy - \int_{\Omega_x}\sum_{j=1}^{N_y}\Big[\Big(\tilde{p}_h^{n+\sigma}\left(x,y_{j+\frac{1}{2}}\right) v\left(x,y_{j+\frac{1}{2}}^-\right)\Big)\\&-\Big(\tilde{p}_h^{n+\sigma}\left(x,y_{j-\frac{1}{2}}\right) v\left(x,y_{j-\frac{1}{2}}^+\right)\Big)\Big] dx\\&=\int_\Omega f^{n+\sigma} v dxdy, \quad \forall v \in V_h^k.\end{aligned} \tag{2.8}$$

To ensure the stability of the LDG scheme, we choose the numerical fluxes as

$$\begin{aligned}&\tilde{u}_h^{n+\sigma}\left(x_{i+\frac{1}{2}},y\right) = u_h^{n+\sigma}\left(x_{i+\frac{1}{2}}^-,y\right), \tilde{q}_h^{n+\sigma}\left(x_{i+\frac{1}{2}},y\right) = q_h^{n+\sigma}\left(x_{i+\frac{1}{2}}^+,y\right),\\&\tilde{u}_h^{n+\sigma}\left(x,y_{j+\frac{1}{2}}\right) = u_h^{n+\sigma}\left(x,y_{j+\frac{1}{2}}^-\right), \tilde{p}_h^{n+\sigma}\left(x,y_{j+\frac{1}{2}}\right) = p_h^{n+\sigma}\left(x,y_{j+\frac{1}{2}}^+\right).\end{aligned} \tag{2.9}$$

3. Stability Analysis

In this section, we derive the stability of the LDG numerical scheme. Before that, we need to introduce the following lemmas.

Lemma 3.1. *(See [25]) For series $\{v^n\}$, the following equality and inequality holds*

$$\int_\Omega \partial_{\Delta t}^{\sigma} v^{n+1} v^{n+\sigma} dxdy \geq \begin{cases} \dfrac{\mathscr{H}[v^{n+1}]-\mathscr{H}[v^n]}{4\Delta t}, & n\geq 1, \\ \dfrac{\|v^1\|^2-\|v^0\|^2}{2\Delta t}, & n=0, \end{cases} \tag{3.1}$$

where $\mathscr{H}[v^{n+1}]=(2\sigma+1)\|v^{n+1}\|^2-(2\sigma-1)\|v^n\|^2+(2\sigma-1)(1+\sigma)\|v^{n+1}-v^n\|^2$ *and*

$$\mathscr{H}[v^{n+1}]\geq \frac{1}{\sigma}\|v^{n+1}\|^2. \tag{3.2}$$

Lemma 3.2. *(See [24, 29]) For* ${}^{\mathscr{F}}g_l^{(n+1)} (0\leq l\leq n, n=0,\cdots,M-1)$*, it holds*

$$\begin{aligned} &{}^{\mathscr{F}}g_n^{(n+1)} > {}^{\mathscr{F}}g_{n-1}^{(n+1)} > {}^{\mathscr{F}}g_{n-2}^{(n+1)} > \cdots > {}^{\mathscr{F}}g_1^{(n+1)} > {}^{\mathscr{F}}g_0^{(n+1)} \geq C^{\mathscr{F}} > 0, \\ &(2\sigma-1){}^{\mathscr{F}}g_n^{(n+1)} - \sigma {}^{\mathscr{F}}g_{n-1}^{(n+1)} \geq 0, \end{aligned} \tag{3.3}$$

where ${}^{\mathscr{F}}g_{-1}^{(n+1)}=0$*, and* $C^{\mathscr{F}}$ *is a positive constant. Then, for series* $\{v^n\}$*, the following inequality holds*

$$\int_\Omega \sum_{l=0}^{n} {}^{\mathscr{F}}g_l^{(n+1)} (v^{l+1}-v^l) v^{n+\sigma} dxdy \geq \frac{1}{2}\sum_{l=0}^{n} {}^{\mathscr{F}}g_l^{(n+1)} \left(\|v^{l+1}\|^2-\|v^l\|^2\right). \tag{3.4}$$

Lemma 3.3. *(See [30]) For* ${}^{\mathscr{F}}g_l^{(n+1)} (0\leq l\leq n, n=0,\cdots,M-1)$*, it holds*

$$\sum_{l=1}^{n-1}\left({}^{\mathscr{F}}g_1^{(l+1)} - {}^{\mathscr{F}}g_0^{(l+1)}\right) \leq \frac{9\varepsilon(n-1)}{4\Gamma(1-\alpha)} + \frac{4-3\alpha}{\Delta t^{\alpha}\Gamma(3-\alpha)}(n-1+\sigma)^{1-\alpha},$$

and

$$\sum_{l=1}^{n-1} {}^{\mathscr{F}}g_0^{(l+1)} \leq \frac{\varepsilon(n-1)}{\Gamma(1-\alpha)} + \frac{(n-1+\sigma)^{1-\alpha}}{\Delta t^{\alpha}\Gamma(2-\alpha)}.$$

Theorem 3.1. *With the periodic or compactly supported boundary conditions and numerical fluxes (2.9), the following stability for the fully discrete LDG system (2.6)-(2.8) holds*

$$\|u_h^n\| \leq C\left(\|u_h^0\| + \max_{1\leq l\leq n}\|f^l\|^2\right), \quad n=1,2,\cdots M,$$

where C is a positive constant independent of Δt and h.

Proof. Adding the three equations (2.6)-(2.8), we have

$$\begin{aligned} &\int_\Omega \partial_{\Delta t}^{\sigma} u_h^{n+1} v dxdy + \int_\Omega {}^{\mathscr{F}}D_t^{\alpha} u_h^{n+\sigma} v dxdy + \int_\Omega q_h^{n+\sigma} w dxdy + \int_\Omega p_h^{n+\sigma}\varphi dxdy \\ &-\gamma_1\sum_{i,j}\int_{I_{i,j}} u_h^{n+\sigma} v_x dxdy - \gamma_2\sum_{i,j}\int_{I_{i,j}} u_h^{n+\sigma} v_y dxdy + \sum_{i,j}\int_{I_{i,j}} u_h^{n+\sigma} w_x dxdy + \sum_{i,j}\int_{I_{i,j}} u_h^{n+\sigma}\varphi_y dxdy \\ &+\sum_{i,j}\int_{I_{i,j}} q_h^{n+\sigma} v_x dxdy + \sum_{i,j}\int_{I_{i,j}} p_h^{n+\sigma} v_y dxdy + \gamma_1\int_{\Omega_y}\sum_{i=1}^{N_x}\left[\left(\tilde{u}_h^{n+\sigma}\left(x_{i+\frac{1}{2}},y\right) v\left(x_{i+\frac{1}{2}}^{-},y\right)\right)\right. \end{aligned}$$

$$-\left(\tilde{u}_h^{n+\sigma}\left(x_{i-\frac{1}{2}},y\right)v\left(x_{i-\frac{1}{2}}^{+},y\right)\right)\Big]dy+\gamma_2\int_{\Omega_x}\sum_{j=1}^{N_y}\Big[\left(\tilde{u}_h^{n+\sigma}\left(x,y_{j+\frac{1}{2}}\right)v\left(x,y_{j+\frac{1}{2}}^{-}\right)\right)$$
$$-\left(\tilde{u}_h^{n+\sigma}\left(x,y_{j-\frac{1}{2}}\right)v\left(x,y_{j-\frac{1}{2}}^{+}\right)\right)\Big]dx-\int_{\Omega_y}\sum_{i=1}^{N_x}\Big[\left(\tilde{u}_h^{n+\sigma}\left(x_{i+\frac{1}{2}},y\right)w\left(x_{i+\frac{1}{2}}^{-},y\right)\right)$$
$$-\left(\tilde{u}_h^{n+\sigma}\left(x_{i-\frac{1}{2}},y\right)w\left(x_{i-\frac{1}{2}}^{+},y\right)\right)\Big]dy-\int_{\Omega_x}\sum_{j=1}^{N_y}\Big[\left(\tilde{u}_h^{n+\sigma}\left(x,y_{j+\frac{1}{2}}\right)\varphi\left(x,y_{j+\frac{1}{2}}^{-}\right)\right)$$
$$-\left(\tilde{u}_h^{n+\sigma}\left(x,y_{j-\frac{1}{2}}\right)\varphi\left(x,y_{j-\frac{1}{2}}^{+}\right)\right)\Big]dx-\int_{\Omega_y}\sum_{i=1}^{N_x}\Big[\left(\tilde{q}_h^{n+\sigma}\left(x_{i+\frac{1}{2}},y\right)v\left(x_{i+\frac{1}{2}}^{-},y\right)\right)$$
$$-\left(\tilde{q}_h^{n+\sigma}\left(x_{i-\frac{1}{2}},y\right)v\left(x_{i-\frac{1}{2}}^{+},y\right)\right)\Big]dy-\int_{\Omega_x}\sum_{j=1}^{N_y}\Big[\left(\tilde{p}_h^{n+\sigma}\left(x,y_{j+\frac{1}{2}}\right)v\left(x,y_{j+\frac{1}{2}}^{-}\right)\right)$$
$$-\left(\tilde{p}_h^{n+\sigma}\left(x,y_{j-\frac{1}{2}}\right)v\left(x,y_{j-\frac{1}{2}}^{+}\right)\right)\Big]dx=\int_{\Omega}f^{n+\sigma}v\,dxdy.$$

Choosing $w=q_h^{n+\sigma}$, $\varphi=p_h^{n+\sigma}$, and $v=u_h^{n+\sigma}$, we can obtain

$$\int_{\Omega}\partial_{\Delta t}^{\sigma}u_h^{n+1}u_h^{n+\sigma}dxdy+\int_{\Omega}{}^{\mathscr{F}}\mathrm{D}_t^{\alpha}u_h^{n+\sigma}u_h^{n+\sigma}dxdy+\int_{\Omega}(q_h^{n+\sigma})^2dxdy+\int_{\Omega}(p_h^{n+\sigma})^2dxdy$$
$$-\gamma_1\sum_{i,j}\int_{I_{i,j}}u_h^{n+\sigma}u_{hx}^{n+\sigma}dxdy-\gamma_2\sum_{i,j}\int_{I_{i,j}}u_h^{n+\sigma}u_{hy}^{n+\sigma}dxdy+\sum_{i,j}\int_{I_{i,j}}u_h^{n+\sigma}q_{hx}^{n+\sigma}dxdy$$
$$+\sum_{i,j}\int_{I_{i,j}}u_h^{n+\sigma}p_{hy}^{n+\sigma}dxdy+\sum_{i,j}\int_{I_{i,j}}q_h^{n+\sigma}u_{hx}^{n+\sigma}dxdy+\sum_{i,j}\int_{I_{i,j}}p_h^{n+\sigma}u_{hy}^{n+\sigma}dxdy$$
$$+\gamma_1\int_{\Omega_y}\sum_{i=1}^{N_x}\Big[\left(\tilde{u}_h^{n+\sigma}\left(x_{i+\frac{1}{2}},y\right)u_h^{n+\sigma}\left(x_{i+\frac{1}{2}}^{-},y\right)\right)$$
$$-\left(\tilde{u}_h^{n+\sigma}\left(x_{i-\frac{1}{2}},y\right)u_h^{n+\sigma}\left(x_{i-\frac{1}{2}}^{+},y\right)\right)\Big]dy+\gamma_2\int_{\Omega_x}\sum_{j=1}^{N_y}\Big[\left(\tilde{u}_h^{n+\sigma}\left(x,y_{j+\frac{1}{2}}\right)u_h^{n+\sigma}\left(x,y_{j+\frac{1}{2}}^{-}\right)\right)$$
$$-\left(\tilde{u}_h^{n+\sigma}\left(x,y_{j-\frac{1}{2}}\right)u_h^{n+\sigma}\left(x,y_{j-\frac{1}{2}}^{+}\right)\right)\Big]dx-\int_{\Omega_y}\sum_{i=1}^{N_x}\Big[\left(\tilde{u}_h^{n+\sigma}\left(x_{i+\frac{1}{2}},y\right)q_h^{n+\sigma}\left(x_{i+\frac{1}{2}}^{-},y\right)\right)$$
$$-\left(\tilde{u}_h^{n+\sigma}\left(x_{i-\frac{1}{2}},y\right)q_h^{n+\sigma}\left(x_{i-\frac{1}{2}}^{+},y\right)\right)\Big]dy-\int_{\Omega_x}\sum_{j=1}^{N_y}\Big[\left(\tilde{u}_h^{n+\sigma}\left(x,y_{j+\frac{1}{2}}\right)p_h^{n+\sigma}\left(x,y_{j+\frac{1}{2}}^{-}\right)\right)$$
$$-\left(\tilde{u}_h^{n+\sigma}\left(x,y_{j-\frac{1}{2}}\right)p_h^{n+\sigma}\left(x,y_{j-\frac{1}{2}}^{+}\right)\right)\Big]dx-\int_{\Omega_y}\sum_{i=1}^{N_x}\Big[\left(\tilde{q}_h^{n+\sigma}\left(x_{i+\frac{1}{2}},y\right)u_h^{n+\sigma}\left(x_{i+\frac{1}{2}}^{-},y\right)\right)$$
$$-\left(\tilde{q}_h^{n+\sigma}\left(x_{i-\frac{1}{2}},y\right)u_h^{n+\sigma}\left(x_{i-\frac{1}{2}}^{+},y\right)\right)\Big]dy-\int_{\Omega_x}\sum_{j=1}^{N_y}\Big[\left(\tilde{p}_h^{n+\sigma}\left(x,y_{j+\frac{1}{2}}\right)u_h^{n+\sigma}\left(x,y_{j+\frac{1}{2}}^{-}\right)\right)$$
$$-\left(\tilde{p}_h^{n+\sigma}\left(x,y_{j-\frac{1}{2}}\right)u_h^{n+\sigma}\left(x,y_{j-\frac{1}{2}}^{+}\right)\right)\Big]dx=\int_{\Omega}f^{n+\sigma}u_h^{n+\sigma}dxdy.$$

According to the Newton-Leibniz formula, we have

$$\begin{aligned}
&\int_{\Omega}\partial_{\Delta t}^{\sigma}u_h^{n+1}u_h^{n+\sigma}dxdy+\int_{\Omega}{}^{\mathscr{F}}D_t^{\alpha}u_h^{n+\sigma}u_h^{n+\sigma}dxdy+\int_{\Omega}(q_h^{n+\sigma})^2dxdy+\int_{\Omega}(p_h^{n+\sigma})^2dxdy\\
&-\gamma_1\sum_{i,j}\int_{I_{i,j}}u_h^{n+\sigma}u_{hx}^{n+\sigma}dxdy-\gamma_2\sum_{i,j}\int_{I_{i,j}}u_h^{n+\sigma}u_{hy}^{n+\sigma}dxdy\\
&+\gamma_1\int_{\Omega_y}\sum_{i=1}^{N_x}\left(\left(\tilde{u}_h^{n+\sigma}\left(x_{i+\frac{1}{2}},y\right)u_h^{n+\sigma}\left(x_{i+\frac{1}{2}}^-,y\right)\right)\right.\\
&\left.-\left(\tilde{u}_h^{n+\sigma}\left(x_{i-\frac{1}{2}},y\right)u_h^{n+\sigma}\left(x_{i-\frac{1}{2}}^+,y\right)\right)\right)dy+\gamma_2\int_{\Omega_x}\sum_{j=1}^{N_y}\left(\left(\tilde{u}_h^{n+\sigma}\left(x,y_{j+\frac{1}{2}}\right)u_h^{n+\sigma}\left(x,y_{j+\frac{1}{2}}^-\right)\right)\right.\\
&\left.-\left(\tilde{u}_h^{n+\sigma}\left(x,y_{j-\frac{1}{2}}\right)u_h^{n+\sigma}\left(x,y_{j-\frac{1}{2}}^+\right)\right)\right)dx+\int_{\Omega_y}\sum_{i=1}^{N_x}\left(\Psi\left(u_h^{n+\sigma}\left(x_{i+\frac{1}{2}},y\right),q_h^{n+\sigma}\left(x_{i+\frac{1}{2}},y\right)\right)\right.\\
&\left.-\Psi\left(u_h^{n+\sigma}\left(x_{i-\frac{1}{2}},y\right),q_h^{n+\sigma}\left(x_{i-\frac{1}{2}},y\right)\right)\right)dy+\int_{\Omega_x}\sum_{j=1}^{N_y}\left(\Phi\left(u_h^{n+\sigma}\left(x,y_{j+\frac{1}{2}}\right),p_h^{n+\sigma}\left(x,y_{j+\frac{1}{2}}\right)\right)\right.\\
&\left.-\Phi\left(u_h^{n+\sigma}\left(x,y_{j-\frac{1}{2}}\right),p_h^{n+\sigma}\left(x,y_{j-\frac{1}{2}}\right)\right)\right)dx+\int_{\Omega_y}\sum_{i=1}^{N_x}\Theta\left(u_h^{n+\sigma}\left(x_{i-\frac{1}{2}},y\right),q_h^{n+\sigma}\left(x_{i-\frac{1}{2}},y\right)\right)dy\\
&+\int_{\Omega_x}\sum_{j=1}^{N_y}\Xi\left(u_h^{n+\sigma}\left(x,y_{j-\frac{1}{2}}\right),p_h^{n+\sigma}\left(x,y_{j-\frac{1}{2}}\right)\right)dx=\int_{\Omega}f^{n+\sigma}u_h^{n+\sigma}dxdy,
\end{aligned}\tag{3.5}$$

where

$$\begin{aligned}
&\Psi\left(u_h^{n+\sigma}\left(x_{i+\frac{1}{2}},y\right),q_h^{n+\sigma}\left(x_{i+\frac{1}{2}},y\right)\right)\\
=&u_h^{n+\sigma}\left(x_{i+\frac{1}{2}}^-,y\right)q_h^{n+\sigma}\left(x_{i+\frac{1}{2}}^-,y\right)-\tilde{u}_h^{n+\sigma}\left(x_{i+\frac{1}{2}},y\right)q_h^{n+\sigma}\left(x_{i+\frac{1}{2}}^-,y\right)\\
&-\tilde{q}_h^{n+\sigma}\left(x_{i+\frac{1}{2}},y\right)u_h^{n+\sigma}\left(x_{i+\frac{1}{2}}^-,y\right),\\
\\
&\Theta\left(u_h^{n+\sigma}\left(x_{i+\frac{1}{2}},y\right),q_h^{n+\sigma}\left(x_{i+\frac{1}{2}},y\right)\right)\\
=&u_h^{n+\sigma}\left(x_{i+\frac{1}{2}}^-,y\right)q_h^{n+\sigma}\left(x_{i+\frac{1}{2}}^-,y\right)-\tilde{u}_h^{n+\sigma}\left(x_{i+\frac{1}{2}},y\right)q_h^{n+\sigma}\left(x_{i+\frac{1}{2}}^-,y\right)\\
&-\tilde{q}_h^{n+\sigma}\left(x_{i+\frac{1}{2}},y\right)u_h^{n+\sigma}\left(x_{i+\frac{1}{2}}^-,y\right)-u_h^{n+\sigma}\left(x_{i+\frac{1}{2}}^+,y\right)q_h^{n+\sigma}\left(x_{i+\frac{1}{2}}^+,y\right)\\
&+\tilde{u}_h^{n+\sigma}\left(x_{i+\frac{1}{2}},y\right)q_h^{n+\sigma}\left(x_{i+\frac{1}{2}}^+,y\right)+\tilde{q}_h^{n+\sigma}\left(x_{i+\frac{1}{2}},y\right)u_h^{n+\sigma}\left(x_{i+\frac{1}{2}}^+,y\right),
\end{aligned}\tag{3.6}$$

$$
\begin{aligned}
&\Phi\left(u_h^{n+\sigma}\left(x,y_{j+\frac{1}{2}}\right),p_h^{n+\sigma}\left(x,y_{j+\frac{1}{2}}\right)\right)\\
=&u_h^{n+\sigma}\left(x,y^-_{j+\frac{1}{2}}\right)p_h^{n+\sigma}\left(x,y^-_{j+\frac{1}{2}}\right)-\tilde{u}_h^{n+\sigma}\left(x,y_{j+\frac{1}{2}}\right)p_h^{n+\sigma}\left(x,y^-_{j+\frac{1}{2}}\right)\\
&-\tilde{p}_h^{n+\sigma}\left(x,y_{j+\frac{1}{2}}\right)u_h^{n+\sigma}\left(x,y^-_{j+\frac{1}{2}}\right),\ \text{and}\\
&\Xi\left(u_h^{n+\sigma}\left(x_{i+\frac{1}{2}},y\right),p_h^{n+\sigma}\left(x_{i+\frac{1}{2}},y\right)\right)\\
=&u_h^{n+\sigma}\left(x,y^-_{j+\frac{1}{2}}\right)p_h^{n+\sigma}\left(x,y^-_{j+\frac{1}{2}}\right)-\tilde{u}_h^{n+\sigma}\left(x,y_{j+\frac{1}{2}}\right)p_h^{n+\sigma}\left(x,y^-_{j+\frac{1}{2}}\right)\\
&-\tilde{p}_h^{n+\sigma}\left(x,y_{j+\frac{1}{2}}\right)u_h^{n+\sigma}\left(x,y^-_{j+\frac{1}{2}}\right)-u_h^{n+\sigma}\left(x,y^+_{j+\frac{1}{2}}\right)p_h^{n+\sigma}\left(x,y^+_{j+\frac{1}{2}}\right)\\
&+\tilde{u}_h^{n+\sigma}\left(x,y_{j+\frac{1}{2}}\right)p_h^{n+\sigma}\left(x,y^+_{j+\frac{1}{2}}\right)+\tilde{p}_h^{n+\sigma}\left(x,y_{j+\frac{1}{2}}\right)u_h^{n+\sigma}\left(x,y^+_{j+\frac{1}{2}}\right).
\end{aligned}
\tag{3.7}
$$

In view of the numerical fluxes (2.9), we easily find that

$$
\Theta\left(u_h^{n+\sigma}\left(x_{i+\frac{1}{2}},y\right),q_h^{n+\sigma}\left(x_{i+\frac{1}{2}},y\right)\right)=0,\ \Xi\left(u_h^{n+\sigma}\left(x_{i+\frac{1}{2}},y\right),p_h^{n+\sigma}\left(x_{i+\frac{1}{2}},y\right)\right)=0,
\tag{3.8}
$$

$$
\begin{aligned}
&-\gamma_1\sum_{i,j}\int_{I_{i,j}}u_h^{n+\sigma}u_{hx}^{n+\sigma}dxdy+\gamma_1\int_{\Omega_y}\sum_{i=1}^{N_x}\left(\left(\tilde{u}_h^{n+\sigma}\left(x_{i+\frac{1}{2}},y\right)u_h^{n+\sigma}\left(x^-_{i+\frac{1}{2}},y\right)\right)\right.\\
&\left.-\left(\tilde{u}_h^{n+\sigma}\left(x_{i-\frac{1}{2}},y\right)u_h^{n+\sigma}\left(x^+_{i-\frac{1}{2}},y\right)\right)\right)dy\\
&=\frac{\gamma_1}{2}\int_{\Omega_y}\sum_{i=1}^{N_x}\left[\left[u_h^{n+\sigma}\left(x_{i-\frac{1}{2}},y\right)\right]\right]^2dy\geq 0,\ \text{and}\\
&-\gamma_2\sum_{i,j}\int_{I_{i,j}}u_h^{n+\sigma}u_{hy}^{n+\sigma}dxdy+\gamma_2\int_{\Omega_x}\sum_{j=1}^{N_y}\left(\left(\tilde{u}_h^{n+\sigma}\left(x,y_{j+\frac{1}{2}}\right)u_h^{n+\sigma}\left(x,y^-_{j+\frac{1}{2}}\right)\right)\right.\\
&\left.-\left(\tilde{u}_h^{n+\sigma}\left(x,y_{j-\frac{1}{2}}\right)u_h^{n+\sigma}\left(x,y^+_{j-\frac{1}{2}}\right)\right)\right)dx\\
&=\frac{\gamma_2}{2}\int_{\Omega_x}\sum_{j=1}^{N_y}\left[\left[u_h^{n+\sigma}\left(x,y_{j-\frac{1}{2}}\right)\right]\right]^2dx\geq 0.
\end{aligned}
\tag{3.9}
$$

With the help of the periodic or compactly supported boundary condition, we have

$$
\begin{aligned}
&\int_{\Omega_y}\sum_{i=1}^{N_x}\left(\Psi\left(u_h^{n+\sigma}\left(x_{i+\frac{1}{2}},y\right),q_h^{n+\sigma}\left(x_{i+\frac{1}{2}},y\right)\right)-\Psi\left(u_h^{n+\sigma}\left(x_{i-\frac{1}{2}},y\right),q_h^{n+\sigma}\left(x_{i-\frac{1}{2}},y\right)\right)\right)dy=0,\\
&\int_{\Omega_x}\sum_{j=1}^{N_y}\left(\Phi\left(u_h^{n+\sigma}\left(x,y_{j+\frac{1}{2}}\right),p_h^{n+\sigma}\left(x,y_{j+\frac{1}{2}}\right)\right)-\Phi\left(u_h^{n+\sigma}\left(x,y_{j-\frac{1}{2}}\right),p_h^{n+\sigma}\left(x,y_{j-\frac{1}{2}}\right)\right)\right)dx=0.
\end{aligned}
\tag{3.10}
$$

First, we discuss the case for $n \geq 1$. Using Lemma 3.1 and (3.4) and substituting (3.6)-(3.10) into (3.5), we have

$$\frac{1}{4\Delta t}\left(\mathscr{H}[u_h^{n+1}]-\mathscr{H}[u_h^n]\right)+\frac{1}{2}\sum_{l=0}^{n}{}^{\mathscr{F}}g_l^{(n+1)}\left(\|u_h^{l+1}\|^2-\|u_h^l\|^2\right)+\|q_h^{n+\sigma}\|^2+\|p_h^{n+\sigma}\|^2$$
$$+\frac{\gamma_1}{2}\int_{\Omega_y}\sum_{i=1}^{N_x}\left[\left[u_h^{n+\sigma}\left(x_{i-\frac{1}{2}},y\right)\right]\right]^2dy+\frac{\gamma_2}{2}\int_{\Omega_x}\sum_{j=1}^{N_y}\left[\left[u_h^{n+\sigma}\left(x,y_{j-\frac{1}{2}}\right)\right]\right]^2dx$$
$$\leq\int_{\Omega}f^{n+\sigma}u_h^{n+\sigma}dxdy.$$

By further calculation, we have

$$\begin{aligned}&\frac{1}{4\Delta t}\mathscr{H}[u_h^{n+1}]+\frac{1}{2}{}^{\mathscr{F}}g_n^{(n+1)}\|u_h^{n+1}\|^2-\frac{1}{2}\sum_{l=1}^{n}\left({}^{\mathscr{F}}g_l^{(n+1)}-{}^{\mathscr{F}}g_{l-1}^{(n+1)}\right)\|u_h^l\|^2\\&\leq\frac{1}{4\Delta t}\mathscr{H}[u_h^n]+\frac{1}{2}{}^{\mathscr{F}}g_0^{(n+1)}\|u_h^0\|^2+\int_{\Omega}f^{n+\sigma}u_h^{n+\sigma}dxdy.\end{aligned}\tag{3.11}$$

Summing (3.11) from $n=1$ to $M-1$ and multiplying $4\Delta t$, we conclude

$$\begin{aligned}&\mathscr{H}[u_h^M]+2\Delta t\sum_{n=1}^{M-1}{}^{\mathscr{F}}g_n^{(n+1)}\|u_h^{n+1}\|^2-2\Delta t\sum_{n=1}^{M-1}\sum_{l=1}^{n}\left({}^{\mathscr{F}}g_l^{(n+1)}-{}^{\mathscr{F}}g_{l-1}^{(n+1)}\right)\|u_h^l\|^2\\&\leq\mathscr{H}[u_h^1]+2\Delta t\sum_{n=1}^{M-1}{}^{\mathscr{F}}g_0^{(n+1)}\|u_h^0\|^2+4\Delta t\sum_{n=1}^{M-1}\int_{\Omega}f^{n+\sigma}u_h^{n+\sigma}dxdy.\end{aligned}$$

Using Cauchy-Schwarz inequality and Young inequality, we obtain

$$\begin{aligned}&\mathscr{H}[u_h^M]+2\Delta t\sum_{n=2}^{M}{}^{\mathscr{F}}g_{n-1}^{(M)}\|u_h^n\|^2\\&\leq\mathscr{H}[u_h^1]+2\Delta t\sum_{n=1}^{M-1}\left({}^{\mathscr{F}}g_1^{(n+1)}-{}^{\mathscr{F}}g_0^{(n+1)}\right)\|u_h^1\|^2+2\Delta t\sum_{n=1}^{M-1}{}^{\mathscr{F}}g_0^{(n+1)}\|u_h^0\|^2\\&\quad+C\Delta t\sum_{n=0}^{M-1}\|f^{n+1}\|^2+C\Delta t\sum_{n=0}^{M-1}\|u_h^{n+1}\|^2.\end{aligned}$$

Using (3.3) and Lemma 3.3, we have

$$\begin{aligned}&\mathscr{H}[u_h^M]+2C^{\mathscr{F}}\Delta t\sum_{n=2}^{M}\|u_h^n\|^2\\&\leq\mathscr{H}[u_h^1]+\left(\frac{9\varepsilon T}{2\Gamma(1-\alpha)}+\frac{2(4-3\alpha)T^{1-\alpha}}{\Gamma(3-\alpha)}\right)\|u_h^1\|^2\\&+\left(\frac{2\varepsilon T}{\Gamma(1-\alpha)}+\frac{2T^{1-\alpha}}{\Gamma(2-\alpha)}\right)\|u_h^0\|^2+C\Delta t\sum_{n=0}^{M-1}\|f^{n+1}\|^2+C\Delta t\sum_{n=0}^{M-1}\|u_h^{n+1}\|^2.\end{aligned}\tag{3.12}$$

Next, we analyze the case for $n=0$. Using Lemma 3.1, (3.4), Cauchy-Schwarz inequality and Young inequality, we can write (3.5) as

$$\begin{aligned}&\frac{1}{2\Delta t}\left(\|u_h^1\|^2-\|u_h^0\|^2\right)+\frac{1}{2}{}^{\mathscr{F}}g_0^{(1)}\left(\|u_h^1\|^2-\|u_h^0\|^2\right)+\|q_h^\sigma\|^2+\|p_h^\sigma\|^2\\&+\frac{\gamma_1}{2}\int_{\Omega_y}\sum_{i=1}^{N_x}\left[\left[u_h^\sigma\left(x_{i-\frac{1}{2}},y\right)\right]\right]^2dy+\frac{\gamma_2}{2}\int_{\Omega_x}\sum_{j=1}^{N_y}\left[\left[u_h^\sigma\left(x,y_{j-\frac{1}{2}}\right)\right]\right]^2dx\\&\leq\int_\Omega f^\sigma u_h^\sigma dxdy.\end{aligned}\tag{3.13}$$

Multiplying (3.13) by $2\Delta t$, and using Cauchy-Schwarz inequality and Young inequality, we have

$$\begin{aligned}&\|u_h^1\|^2+C^{\mathscr{F}}\Delta t\|u_h^1\|^2\\&\leq\|u_h^0\|^2+{}^{\mathscr{F}}g_0^{(1)}\Delta t\|u_h^0\|^2+C\Delta t(\|f^0\|^2+\|f^1\|^2)+C\Delta t(\|u_h^0\|^2+\|u_h^1\|^2).\end{aligned}$$

Using the discrete Gronwall inequality, we have

$$\|u_h^1\|^2+C^{\mathscr{F}}\Delta t\|u_h^1\|^2\leq C\|u_h^0\|^2+C\Delta t(\|f^0\|^2+\|f^1\|^2).\tag{3.14}$$

Noting that $\mathscr{H}[u_h^1]\leq C\|u_h^1\|^2$, and substituting (3.14) into (3.12), we have

$$\mathscr{H}[u_h^M]+2C^{\mathscr{F}}\Delta t\sum_{n=2}^{M}\|u_h^n\|^2\leq C\|u_h^0\|^2+C\Delta t\sum_{n=0}^{M}\|f^n\|^2+C\Delta t\sum_{n=0}^{M}\|u_h^n\|^2.$$

Using (3.2) and the discrete Gronwall inequality for sufficiently small Δt, we have

$$\|u_h^M\|^2\leq C\|u_h^0\|^2+C\Delta t\sum_{n=0}^{M}\|f^n\|^2.$$

Finally, we have the proof of stability. □

4. Error Analysis

To derive the error estimate of our LDG scheme, we first consider the projection operator in the one-dimensional case. We introduce the standard L^2-projection of a function $\omega(x)\in L^2(I_i)$ with continuous derivative of $k+1$ into finite element space V_h^k, denoted by $\mathscr{P}$, i.e., for each i,

$$\int_{I_i}\left(\mathscr{P}w(x)-w(x)\right)v(x)\,dx=0,\forall v\in P^k(I_i),$$

and special projection $\mathscr{P}^\pm$ into V_h^k, i.e., for each I_i,

$$\begin{aligned}&\int_{I_i}\left(\mathscr{P}^+w(x)-w(x)\right)v(x)\,dx=0,\forall v\in P^{k-1}(I_i),\mathscr{P}^+w\left(x_{i-\frac{1}{2}}^+\right)=w\left(x_{i-\frac{1}{2}}\right),\\&\int_{I_i}\left(\mathscr{P}^-w(x)-w(x)\right)v(x)\,dx=0,\forall v\in P^{k-1}(I_i),\mathscr{P}^-w\left(x_{i+\frac{1}{2}}^-\right)=w\left(x_{i+\frac{1}{2}}\right).\end{aligned}$$

Based on the above projections, we give the projections in [35] to prove the error estimates of two-dimensional problems in Cartesian meshes. On the spatial domain $\bar{\Omega}_x\times\bar{\Omega}_y$, we define

$$\mathbb{P}\omega=\mathscr{P}_x\otimes\mathscr{P}_y\omega,\mathbb{P}^\pm\omega=\mathscr{P}_x^\pm\otimes\mathscr{P}_y^\pm\omega,$$

where the subscripts indicate the application of the one-dimensional operators $\mathscr{P}$ or $\mathscr{P}^{\pm}$ with respect to the corresponding variable. The projections $\mathbb{P}^{\pm}$ satisfy

$$\begin{aligned} &\int_{I_i}\int_{J_j}(\mathbb{P}^{\pm}\omega(x,y)-\omega(x,y))v(x,y)dydx=0,\\ &\forall v\in(P^{k-1}(I_i)\otimes P^k(J_j))\cup(P^k(I_i)\otimes P^{k-1}(J_j)). \end{aligned} \tag{4.1}$$

Projection $\mathbb{P}^{+}$ also satisfies

$$\begin{aligned} &\int_{J_j}(\mathbb{P}^{+}\omega(x^+_{i-\frac{1}{2}},y)-\omega(x^+_{i-\frac{1}{2}},y))v(x^+_{i-\frac{1}{2}},y)dy=0, \quad \forall v\in Q^k(I_i\otimes J_j),\\ &\int_{I_i}(\mathbb{P}^{+}\omega(x,y^+_{j-\frac{1}{2}})-\omega(x,y^+_{j-\frac{1}{2}}))v(x,y^+_{j-\frac{1}{2}})dx=0, \quad \forall v\in Q^k(I_i\otimes J_j). \end{aligned} \tag{4.2}$$

Projection $\mathbb{P}^{-}$ also satisfies

$$\begin{aligned} &\int_{J_j}(\mathbb{P}^{-}\omega(x^-_{i-\frac{1}{2}},y)-\omega(x^-_{i-\frac{1}{2}},y))v(x^-_{i-\frac{1}{2}},y)dy=0, \quad \forall v\in Q^k(I_i\otimes J_j),\\ &\int_{I_i}(\mathbb{P}^{-}\omega(x,y^-_{j-\frac{1}{2}})-\omega(x,y^-_{j-\frac{1}{2}}))v(x,y^-_{j-\frac{1}{2}})dx=0, \quad \forall v\in Q^k(I_i\otimes J_j). \end{aligned} \tag{4.3}$$

For the projection operators above, we can see the following approximation result [35]

$$\|\omega^e\|+h\|\omega^e\|_\infty+h^{\frac{1}{2}}\|\omega^e\|_{\Gamma_h}\le Ch^{k+1}, \tag{4.4}$$

where $\omega^e=\mathbb{P}\omega(x)-\omega(x)$ or $\omega^e=\mathbb{P}^{\pm}\omega(x)-\omega(x)$. The positive constant C is independent of h. Γ_h denotes the set of boundary points of all elements $I_i\otimes J_j$.

To simplify error analysis, we write the error as

$$\begin{aligned} e_u^{n+1}&=u^{n+1}-u_h^{n+1}=\mathbb{P}^-u^{n+1}-u_h^{n+1}+u^{n+1}-\mathbb{P}^-u^{n+1}=\xi_u^{n+1}+\eta_u^{n+1},\\ e_q^{n+1}&=q^{n+1}-q_h^{n+1}=\mathbb{P}^+q^{n+1}-q_h^{n+1}+q^{n+1}-\mathbb{P}^+q^{n+1}=\xi_q^{n+1}+\eta_q^{n+1},\\ e_p^{n+1}&=p^{n+1}-p_h^{n+1}=\mathbb{P}^+p^{n+1}-p_h^{n+1}+p^{n+1}-\mathbb{P}^+p^{n+1}=\xi_p^{n+1}+\eta_p^{n+1}. \end{aligned} \tag{4.5}$$

Subtracting (2.6)-(2.8) with (2.3)-(2.5), and using the numerical fluxes (2.9) at $t=t_{n+\sigma}$, we have the error equation

$$\begin{aligned} &\int_\Omega e_q^{n+\sigma}wdxdy+\sum_{i,j}\int_{I_{i,j}}e_u^{n+\sigma}w_xdxdy-\int_{\Omega_y}\sum_{i=1}^{N_x}\left[\left(e_u^{n+\sigma}\left(x^-_{i+\frac{1}{2}},y\right)w\left(x^-_{i+\frac{1}{2}},y\right)\right)\right.\\ &\left.-\left(e_u^{n+\sigma}\left(x^-_{i-\frac{1}{2}},y\right)w\left(x^+_{i-\frac{1}{2}},y\right)\right)\right]dy=\int_\Omega R_1^{n+\sigma}wdxdy, \end{aligned} \tag{4.6}$$

$$\begin{aligned} &\int_\Omega e_p^{n+\sigma}\varphi dxdy+\sum_{i,j}\int_{I_{i,j}}e_u^{n+\sigma}\varphi_ydxdy-\int_{\Omega_x}\sum_{j=1}^{N_y}\left[\left(e_u^{n+\sigma}\left(x,y^-_{j+\frac{1}{2}}\right)\varphi\left(x,y^-_{j+\frac{1}{2}}\right)\right)\right.\\ &\left.-\left(e_u^{n+\sigma}\left(x,y^-_{j-\frac{1}{2}}\right)\varphi\left(x,y^+_{j-\frac{1}{2}}\right)\right)\right]dx=\int_\Omega R_2^{n+\sigma}\varphi dxdy, \end{aligned} \tag{4.7}$$

and

$$\begin{aligned}
&\int_\Omega \partial_{\Delta t}^\sigma e_u^{n+1} v dxdy + \int_\Omega {}^{\mathscr{F}}D_t^\alpha e_u^{n+\sigma} v dxdy - \gamma_1 \sum_{i,j} \int_{I_{i,j}} e_u^{n+\sigma} v_x dxdy - \gamma_2 \sum_{i,j} \int_{I_{i,j}} e_u^{n+\sigma} v_y dxdy \\
&+ \sum_{i,j} \int_{I_{i,j}} e_q^{n+\sigma} v_x dxdy + \sum_{i,j} \int_{I_{i,j}} e_p^{n+\sigma} v_y dxdy + \gamma_1 \int_{\Omega_y} \sum_{i=1}^{N_x} \left[\left(e_u^{n+\sigma} \left(x_{i+\frac{1}{2}}^-, y \right) v \left(x_{i+\frac{1}{2}}^-, y \right) \right) \right. \\
&- \left. \left(e_u^{n+\sigma} \left(x_{i-\frac{1}{2}}^-, y \right) v \left(x_{i-\frac{1}{2}}^+, y \right) \right) \right] dy + \gamma_2 \int_{\Omega_x} \sum_{j=1}^{N_y} \left[\left(e_u^{n+\sigma} \left(x, y_{j+\frac{1}{2}}^- \right) v \left(x, y_{j+\frac{1}{2}}^- \right) \right) \right. \\
&- \left. \left(e_u^{n+\sigma} \left(x, y_{j-\frac{1}{2}}^- \right) v \left(x, y_{j-\frac{1}{2}}^+ \right) \right) \right] dx - \int_{\Omega_y} \sum_{i=1}^{N_x} \left[\left(e_q^{n+\sigma} \left(x_{i+\frac{1}{2}}^+, y \right) v \left(x_{i+\frac{1}{2}}^-, y \right) \right) \right. \\
&- \left. \left(e_q^{n+\sigma} \left(x_{i-\frac{1}{2}}^+, y \right) v \left(x_{i-\frac{1}{2}}^+, y \right) \right) \right] dy - \int_{\Omega_x} \sum_{j=1}^{N_y} \left[\left(e_p^{n+\sigma} \left(x, y_{j+\frac{1}{2}}^+ \right) v \left(x, y_{j+\frac{1}{2}}^- \right) \right) \right. \\
&- \left. \left(e_p^{n+\sigma} \left(x, y_{j-\frac{1}{2}}^+ \right) v \left(x, y_{j-\frac{1}{2}}^+ \right) \right) \right] dx = \int_\Omega R_3^{n+\sigma} v dxdy + \int_\Omega R_4^{n+\sigma} v dxdy + \int_\Omega R_5^{n+\sigma} v dxdy.
\end{aligned} \tag{4.8}$$

Theorem 4.1. *Suppose problem (1.1)-(1.2) has a unique smooth solution. Let u^n and u_h^n be the exact and numerical solutions to system (2.3)-(2.5) and fully discrete LDG numerical scheme (2.6)-(2.8), respectively. Then $\|u^n - u_h^n\| \leq C\left(h^{k+1} + \Delta t^2 + \varepsilon\right)$, where the constant C is independent of h and Δt.*

Proof. Substituting (4.5) into (4.6)-(4.8), we have

$$\begin{aligned}
&\int_\Omega \xi_q^{n+\sigma} w dxdy + \sum_{i,j} \int_{I_{i,j}} \xi_u^{n+\sigma} w_x dxdy - \int_{\Omega_y} \sum_{i=1}^{N_x} \left[\left(\xi_u^{n+\sigma} \left(x_{i+\frac{1}{2}}^-, y \right) w \left(x_{i+\frac{1}{2}}^-, y \right) \right) \right. \\
&- \left. \left(\xi_u^{n+\sigma} \left(x_{i-\frac{1}{2}}^-, y \right) w \left(x_{i-\frac{1}{2}}^+, y \right) \right) \right] dy \\
=& - \int_\Omega \eta_q^{n+\sigma} w dxdy - \sum_{i,j} \int_{I_{i,j}} \eta_u^{n+\sigma} w_x dxdy + \int_{\Omega_y} \sum_{i=1}^{N_x} \left[\left(\eta_u^{n+\sigma} \left(x_{i+\frac{1}{2}}^-, y \right) w \left(x_{i+\frac{1}{2}}^-, y \right) \right) \right. \\
&- \left. \left(\eta_u^{n+\sigma} \left(x_{i-\frac{1}{2}}^-, y \right) w \left(x_{i-\frac{1}{2}}^+, y \right) \right) \right] dy + \int_\Omega R_1^{n+\sigma} w dxdy,
\end{aligned} \tag{4.9}$$

$$\begin{aligned}
&\int_\Omega \xi_p^{n+\sigma} \varphi dxdy + \sum_{i,j} \int_{I_{i,j}} \xi_u^{n+\sigma} \varphi_y dxdy - \int_{\Omega_x} \sum_{j=1}^{N_y} \left[\left(\xi_u^{n+\sigma} \left(x, y_{j+\frac{1}{2}}^- \right) \varphi \left(x, y_{j+\frac{1}{2}}^- \right) \right) \right. \\
&- \left. \left(\xi_u^{n+\sigma} \left(x, y_{j-\frac{1}{2}}^- \right) \varphi \left(x, y_{j-\frac{1}{2}}^+ \right) \right) \right] dx \\
=& - \int_\Omega \eta_p^{n+\sigma} \varphi dxdy - \sum_{i,j} \int_{I_{i,j}} \eta_u^{n+\sigma} \varphi_y dxdy + \int_{\Omega_x} \sum_{j=1}^{N_y} \left[\left(\eta_u^{n+\sigma} \left(x, y_{j+\frac{1}{2}}^- \right) \varphi \left(x, y_{j+\frac{1}{2}}^- \right) \right) \right. \\
&- \left. \left(\eta_u^{n+\sigma} \left(x, y_{j-\frac{1}{2}}^- \right) \varphi \left(x, y_{j-\frac{1}{2}}^+ \right) \right) \right] dx + \int_\Omega R_2^{n+\sigma} \varphi dxdy,
\end{aligned} \tag{4.10}$$

and

$$\begin{aligned}
&\int_\Omega \partial_{\Delta t}^\sigma \xi_u^{n+1} v dxdy + \int_\Omega {}^{\mathscr{F}}D_t^\alpha \xi_u^{n+\sigma} v dxdy - \gamma_1 \sum_{i,j}\int_{I_{i,j}} \xi_u^{n+\sigma} v_x dxdy - \gamma_2 \sum_{i,j}\int_{I_{i,j}} \xi_u^{n+\sigma} v_y dxdy \\
&+\sum_{i,j}\int_{I_{i,j}} \xi_q^{n+\sigma} v_x dxdy + \sum_{i,j}\int_{I_{i,j}} \xi_p^{n+\sigma} v_y dxdy + \gamma_1 \int_{\Omega_y}\sum_{i=1}^{N_x}\left[\left(\xi_u^{n+\sigma}\left(x_{i+\frac12}^-,y\right) v\left(x_{i+\frac12}^-,y\right)\right)\right. \\
&\left.-\left(\xi_u^{n+\sigma}\left(x_{i-\frac12}^-,y\right) v\left(x_{i-\frac12}^+,y\right)\right)\right] dy + \gamma_2 \int_{\Omega_x}\sum_{j=1}^{N_y}\left[\left(\xi_u^{n+\sigma}\left(x,y_{j+\frac12}^-\right) v\left(x,y_{j+\frac12}^-\right)\right)\right. \\
&\left.-\left(\xi_u^{n+\sigma}\left(x,y_{j-\frac12}^-\right) v\left(x,y_{j-\frac12}^+\right)\right)\right] dx - \int_{\Omega_y}\sum_{i=1}^{N_x}\left[\left(\xi_q^{n+\sigma}\left(x_{i+\frac12}^+,y\right) v\left(x_{i+\frac12}^-,y\right)\right)\right. \\
&\left.-\left(\xi_q^{n+\sigma}\left(x_{i-\frac12}^+,y\right) v\left(x_{i-\frac12}^+,y\right)\right)\right] dy - \int_{\Omega_x}\sum_{j=1}^{N_y}\left[\left(\xi_p^{n+\sigma}\left(x,y_{j+\frac12}^+\right) v\left(x,y_{j+\frac12}^-\right)\right)\right. \\
&\left.-\left(\xi_p^{n+\sigma}\left(x,y_{j-\frac12}^+\right) v\left(x,y_{j-\frac12}^+\right)\right)\right] dx \\
=&-\int_\Omega \partial_{\Delta t}^\sigma \eta_u^{n+1} v dxdy - \int_\Omega {}^{\mathscr{F}}D_t^\alpha \eta_u^{n+\sigma} v dxdy + \gamma_1 \sum_{i,j}\int_{I_{i,j}} \eta_u^{n+\sigma} v_x dxdy + \gamma_2 \sum_{i,j}\int_{I_{i,j}} \eta_u^{n+\sigma} v_y dxdy \\
&-\sum_{i,j}\int_{I_{i,j}} \eta_q^{n+\sigma} v_x dxdy - \sum_{i,j}\int_{I_{i,j}} \eta_p^{n+\sigma} v_y dxdy - \gamma_1 \int_{\Omega_y}\sum_{i=1}^{N_x}\left[\left(\eta_u^{n+\sigma}\left(x_{i+\frac12}^-,y\right) v\left(x_{i+\frac12}^-,y\right)\right)\right. \\
&\left.-\left(\eta_u^{n+\sigma}\left(x_{i-\frac12}^-,y\right) v\left(x_{i-\frac12}^+,y\right)\right)\right] dy - \gamma_2 \int_{\Omega_x}\sum_{j=1}^{N_y}\left[\left(\eta_u^{n+\sigma}\left(x,y_{j+\frac12}^-\right) v\left(x,y_{j+\frac12}^-\right)\right)\right. \\
&\left.-\left(\eta_u^{n+\sigma}\left(x,y_{j-\frac12}^-\right) v\left(x,y_{j-\frac12}^+\right)\right)\right] dx + \int_{\Omega_y}\sum_{i=1}^{N_x}\left[\left(\eta_q^{n+\sigma}\left(x_{i+\frac12}^+,y\right) v\left(x_{i+\frac12}^-,y\right)\right)\right. \\
&\left.-\left(\eta_q^{n+\sigma}\left(x_{i-\frac12}^+,y\right) v\left(x_{i-\frac12}^+,y\right)\right)\right] dy + \int_{\Omega_x}\sum_{j=1}^{N_y}\left[\left(\eta_p^{n+\sigma}\left(x,y_{j+\frac12}^+\right) v\left(x,y_{j+\frac12}^-\right)\right)\right. \\
&\left.-\left(\eta_p^{n+\sigma}\left(x,y_{j-\frac12}^+\right) v\left(x,y_{j-\frac12}^+\right)\right)\right] dx + \int_\Omega R_3^{n+\sigma} v dxdy + \int_\Omega R_4^{n+\sigma} v dxdy + \int_\Omega R_5^{n+\sigma} v dxdy.
\end{aligned} \tag{4.11}$$

Adding (4.9)-(4.11) together, taking $w=\xi_q^{n+\sigma}$, $\varphi=\xi_p^{n+\sigma}$, $v=\xi_u^{n+\sigma}$, and using properties of the projections (4.1)-(4.3), we can obtain

$$\begin{aligned}
&\int_\Omega \partial_{\Delta t}^\sigma \xi_u^{n+1}\xi_u^{n+\sigma} dxdy + \int_\Omega {}^{\mathscr{F}}D_t^\alpha \xi_u^{n+\sigma}\xi_u^{n+\sigma} dxdy + \int_\Omega (\xi_q^{n+\sigma})^2 dxdy + \int_\Omega (\xi_p^{n+\sigma})^2 dxdy \\
&+\frac{\gamma_1}{2}\int_{\Omega_y}\sum_{i=1}^{N_x}\left[\left[\xi_u^{n+\sigma}\left(x_{i-\frac12},y\right)\right]\right]^2 dy + \frac{\gamma_2}{2}\int_{\Omega_x}\sum_{j=1}^{N_y}\left[\left[\xi_u^{n+\sigma}\left(x,y_{j-\frac12}\right)\right]\right]^2 dx
\end{aligned}$$

$$
\begin{aligned}
=&-\int_\Omega \partial_{\Delta t}^{\sigma}\eta_u^{n+1}\xi_u^{n+\sigma}dxdy-\int_\Omega {}^{\mathscr{F}}D_t^{\alpha}\eta_u^{n+\sigma}\xi_u^{n+\sigma}dxdy-\int_\Omega \eta_q^{n+\sigma}\xi_q^{n+\sigma}dxdy\\
&-\int_\Omega \eta_p^{n+\sigma}\xi_p^{n+\sigma}dxdy+\int_\Omega R_1^{n+\sigma}\xi_q^{n+\sigma}dxdy+\int_\Omega R_2^{n+\sigma}\xi_p^{n+\sigma}dxdy\\
&+\int_\Omega R_3^{n+\sigma}\xi_u^{n+\sigma}dxdy+\int_\Omega R_4^{n+\sigma}\xi_u^{n+\sigma}dxdy+\int_\Omega R_5^{n+\sigma}\xi_u^{n+\sigma}dxdy\\
=&\Upsilon_1+\Upsilon_2+\Upsilon_3+\Upsilon_4.
\end{aligned}
\tag{4.12}
$$

Now we discuss the case for $n\geq 1$. For Υ_1, using Cauchy-Schwarz inequality and Young inequality, we have

$$
\Upsilon_1=-\int_\Omega \partial_{\Delta t}^{\sigma}\eta_u^{n+1}\xi_u^{n+\sigma}dxdy\leq \frac{C}{\Delta t}\int_{t_{n-1}}^{t_{n+1}}\|(\eta_u)_t\|^2ds+C\|\xi_u^{n+\sigma}\|^2. \tag{4.13}
$$

To estimate Υ_2, we first have

$$
\begin{aligned}
&{}_0^CD_t^{\alpha}\left(u(t_{n+\sigma})-\mathbb{P}^-u(t_{n+\sigma})\right)\\
\leq&\frac{1}{\Gamma(1-\alpha)}\int_0^{t_{n+\sigma}}\left|u_s(x,y,s)-\mathbb{P}^-u_s(x,y,s)\right|(t_{n+\sigma}-s)^{-\alpha}ds\\
\leq&\frac{1}{\Gamma(1-\alpha)}\max_{t_0\leq s\leq t_{n+\sigma}}\left|u_s(x,y,s)-\mathbb{P}^-u_s(x,y,s)\right|\int_0^{t_{n+\sigma}}(t_{n+\sigma}-s)^{-\alpha}ds\\
\leq&\frac{t_{n+\sigma}^{1-\alpha}}{\Gamma(2-\alpha)}\max_{t_0\leq s\leq t_{n+\sigma}}\left|u_s(x,y,s)-\mathbb{P}^-u_s(x,y,s)\right|.
\end{aligned}
\tag{4.14}
$$

Then using (4.4) and (4.14), we have

$$
\left\|{}_0^CD_t^{\alpha}\left(u(t_{n+\sigma})-\mathbb{P}^-u(t_{n+\sigma})\right)\right\|\leq \frac{t_{n+\sigma}^{1-\alpha}}{\Gamma(2-\alpha)}\max_{t_0\leq s\leq t_{n+\sigma}}\left\|u_s(x,y,s)-\mathbb{P}^-u_s(x,y,s)\right\|\leq Ch^{k+1}. \tag{4.15}
$$

For Υ_2, using (4.14), (4.15), Cauchy-Schwarz inequality, and Young inequality, we have

$$
\begin{aligned}
\Upsilon_2=&-\int_\Omega\left({}_0^CD_t^{\alpha}\eta_u^{n+\sigma}-O(\Delta t^{3-\alpha}+\varepsilon)\right)\xi_u^{n+\sigma}dxdy\\
\leq& C\left(\left\|{}_0^CD_t^{\alpha}\left(u(t_{n+\sigma})-\mathbb{P}^-u(t_{n+\sigma})\right)\right\|^2+\Delta t^{2(3-\alpha)}+\varepsilon^2+\|\xi_u^{n+\sigma}\|^2\right)\\
\leq& C(h^{2(k+1)}+\Delta t^{2(3-\alpha)}+\varepsilon^2+\|\xi_u^{n+\sigma}\|^2),
\end{aligned}
\tag{4.16}
$$

For Υ_3, using (4.4), Cauchy-Schwarz inequality and Young inequality, we can get

$$
\begin{aligned}
\Upsilon_3=&-\int_\Omega \eta_q^{n+\sigma}\xi_q^{n+\sigma}dxdy-\int_\Omega \eta_p^{n+\sigma}\xi_p^{n+\sigma}dxdy\\
\leq&\|\eta_q^{n+\sigma}\|^2+\|\eta_p^{n+\sigma}\|^2+\frac{1}{4}\left(\|\xi_q^{n+\sigma}\|^2+\|\xi_p^{n+\sigma}\|^2\right)\\
\leq& Ch^{2(k+1)}+\frac{1}{4}\left(\|\xi_q^{n+\sigma}\|^2+\|\xi_p^{n+\sigma}\|^2\right).
\end{aligned}
\tag{4.17}
$$

For Υ_4, using (2.2), Cauchy-Schwarz inequality and Young inequality, we have

$$\begin{aligned}\Upsilon_4 =& \int_\Omega R_1^{n+\sigma}\xi_q^{n+\sigma}dxdy + \int_\Omega R_2^{n+\sigma}\xi_p^{n+\sigma}dxdy \\ &+ \int_\Omega R_3^{n+\sigma}\xi_u^{n+\sigma}dxdy + \int_\Omega R_4^{n+\sigma}\xi_u^{n+\sigma}dxdy + \int_\Omega R_5^{n+\sigma}\xi_u^{n+\sigma}dxdy \\ \leq& C\left(\Delta t^4 + \varepsilon^2 + \|\xi_u^{n+\sigma}\|^2\right) + \frac{1}{4}\left(\|\xi_q^{n+\sigma}\|^2 + \|\xi_p^{n+\sigma}\|^2\right).\end{aligned} \tag{4.18}$$

Substituting (4.13)-(4.18) into (4.12), and using Lemma 3.1, (3.4) and (3.9), we have

$$\begin{aligned}&\frac{1}{4\Delta t}\mathscr{H}[\xi_u^{n+1}] + \frac{1}{2}{}^{\mathscr{F}}g_n^{(n+1)}\|\xi_u^{n+1}\|^2 - \frac{1}{2}\sum_{l=1}^{n}\left({}^{\mathscr{F}}g_l^{(n+1)} - {}^{\mathscr{F}}g_{l-1}^{(n+1)}\right)\|\xi_u^l\|^2 \\ &\leq \frac{1}{4\Delta t}\mathscr{H}[\xi_u^n] + \frac{1}{2}{}^{\mathscr{F}}g_0^{(n+1)}\|\xi_u^0\|^2 + \frac{C}{\Delta t}\int_{t_{n-1}}^{t_{n+1}}\|(\eta_u)_t\|^2ds \\ &+ C\|\xi_u^{n+\sigma}\|^2 + C\left(h^{2(k+1)} + \Delta t^4 + \varepsilon^2\right).\end{aligned} \tag{4.19}$$

Summing with respect to n from 1 to $M-1$, and multiplying (4.19) by $4\Delta t$, we have

$$\begin{aligned}&\mathscr{H}[\xi_u^M] + 2\Delta t\sum_{n=1}^{M-1}{}^{\mathscr{F}}g_n^{(n+1)}\|\xi_u^{n+1}\|^2 - 2\Delta t\sum_{n=1}^{M-1}\sum_{l=1}^{n}\left({}^{\mathscr{F}}g_l^{(n+1)} - {}^{\mathscr{F}}g_{l-1}^{(n+1)}\right)\|\xi_u^l\|^2 \\ &\leq \mathscr{H}[\xi_u^1] + 2\Delta t\sum_{n=1}^{M-1}{}^{\mathscr{F}}g_0^{(n+1)}\|\xi_u^0\|^2 + C\int_{t_0}^{t_M}\|(\eta_u)_t\|^2ds \\ &+ C\Delta t\sum_{n=1}^{M-1}\|\xi_u^{n+\sigma}\|^2 + C\Delta t\sum_{n=1}^{M-1}\left(h^{2(k+1)} + \Delta t^4 + \varepsilon^2\right).\end{aligned}$$

After further calculation, we have

$$\begin{aligned}&\mathscr{H}[u_h^M] + 2\Delta t\sum_{n=2}^{M}{}^{\mathscr{F}}g_{n-1}^{(M)}\|\xi_u^n\|^2 \\ &\leq \mathscr{H}[u_h^1] + 2\Delta t\sum_{n=1}^{M-1}\left({}^{\mathscr{F}}g_1^{(n+1)} - {}^{\mathscr{F}}g_0^{(n+1)}\right)\|\xi_u^1\|^2 + 2\Delta t\sum_{n=1}^{M-1}{}^{\mathscr{F}}g_0^{(n+1)}\|\xi_u^0\|^2 \\ &+ C\int_{t_0}^{t_M}\|(\eta_u)_t\|^2ds + C\Delta t\sum_{n=1}^{M-1}\|\xi_u^{n+\sigma}\|^2 + C\Delta t\sum_{n=1}^{M-1}\left(h^{2(k+1)} + \Delta t^4 + \varepsilon^2\right).\end{aligned}$$

Using (3.3) and Lemmas 3.3, we have

$$\begin{aligned}\mathscr{H}[\xi_u^M] + 2C^{\mathscr{F}}\Delta t\sum_{n=2}^{M}\|\xi_u^n\|^2 \leq& \mathscr{H}[\xi_u^1] + \left(\frac{9\varepsilon T}{2\Gamma(1-\alpha)} + \frac{2(4-3\alpha)T^{1-\alpha}}{\Gamma(3-\alpha)}\right)\|\xi_u^1\|^2 \\ &+ \left(\frac{2\varepsilon T}{\Gamma(1-\alpha)} + \frac{2T^{1-\alpha}}{\Gamma(2-\alpha)}\right)\|\xi_u^0\|^2 + C\int_{t_0}^{t_M}\|(\eta_u)_t\|^2ds \\ &+ C\Delta t\sum_{n=1}^{M}\|\xi_u^n\|^2 + C\Delta t\sum_{n=1}^{M-1}\left(h^{2(k+1)} + \Delta t^4 + \varepsilon^2\right).\end{aligned} \tag{4.20}$$

In (4.12), we take $n=0$ to obtain

$$\begin{aligned}&\int_\Omega \partial_{\Delta t}^{\sigma}\xi_u^1\xi_u^\sigma dxdy+\int_\Omega {}^{\mathscr{F}}D_t^\alpha \xi_u^\sigma\xi_u^\sigma dxdy+\int_\Omega(\xi_q^\sigma)^2dxdy+\int_\Omega(\xi_p^\sigma)^2dxdy\\&+\frac{\gamma_1}{2}\int_{\Omega_y}\sum_{i=1}^{N_x}\left[\left[\xi_u^\sigma\left(x_{i-\frac{1}{2}},y\right)\right]\right]^2dy+\frac{\gamma_2}{2}\int_{\Omega_x}\sum_{j=1}^{N_y}\left[\left[\xi_u^\sigma\left(x,y_{j-\frac{1}{2}}\right)\right]\right]^2dx\\&=-\int_\Omega\partial_{\Delta t}^{\sigma}\eta_u^1\xi_u^\sigma dxdy-\int_\Omega{}^{\mathscr{F}}D_t^\alpha\eta_u^\sigma\xi_u^\sigma dxdy-\int_\Omega\eta_q^\sigma\xi_q^\sigma dxdy\\&\quad-\int_\Omega\eta_p^\sigma\xi_p^\sigma dxdy+\int_\Omega R_1^\sigma\xi_q^\sigma dxdy+\int_\Omega R_2^\sigma\xi_p^\sigma dxdy\\&\quad+\int_\Omega R_3^\sigma\xi_u^\sigma dxdy+\int_\Omega R_4^\sigma\xi_u^\sigma dxdy+\int_\Omega R_5^\sigma\xi_u^\sigma dxdy.\end{aligned}$$

Using (3.1), (3.4), and multiplying both sides by $2\Delta t$, we have

$$\begin{aligned}&\|\xi_u^1\|^2+\Delta t^{\mathscr{F}}g_0^{(1)}\|\xi_u^1\|^2+2\Delta t\|\xi_q^\sigma\|^2+2\Delta t\|\xi_p^\sigma\|^2\\&\le\|\xi_u^0\|^2+\Delta t^{\mathscr{F}}g_0^{(1)}\|\xi_u^0\|^2-2\Delta t\int_\Omega\partial_{\Delta t}^{\sigma}\eta_u^1\xi_u^\sigma dxdy-2\Delta t\int_\Omega{}^{\mathscr{F}}D_t^\alpha\eta_u^\sigma\xi_u^\sigma dxdy\\&-2\Delta t\int_\Omega\eta_q^\sigma\xi_q^\sigma dxdy-2\Delta t\int_\Omega\eta_p^\sigma\xi_p^\sigma dxdy+2\Delta t\int_\Omega R_1^\sigma\xi_q^\sigma dxdy+2\Delta t\int_\Omega R_2^\sigma\xi_p^\sigma dxdy\\&+2\Delta t\int_\Omega R_3^\sigma\xi_u^\sigma dxdy+2\Delta t\int_\Omega R_4^\sigma\xi_u^\sigma dxdy+2\Delta t\int_\Omega R_5^\sigma\xi_u^\sigma dxdy.\end{aligned}$$

Using (4.4), Cauchy inequality and Young inequality, we have

$$\begin{aligned}&\|\xi_u^1\|^2+C^{\mathscr{F}}\Delta t\|\xi_u^1\|^2+2\Delta t\|\xi_q^\sigma\|^2+2\Delta t\|\xi_p^\sigma\|^2\\&\le Ch^{2(k+1)}+\frac{1}{2}\|\xi_u^1\|^2+C\Delta t\|\xi_u^\sigma\|^2+\Delta t\|\xi_q^\sigma\|^2+\Delta t\|\xi_p^\sigma\|^2+C(\Delta t^4+\Delta t^{2(3-\alpha)}+\varepsilon^2).\end{aligned}$$

Further, we have $\|\xi_u^1\|^2\le C(h^{2(k+1)}+\Delta t^4+\varepsilon^2)$, which together with (4.20) yields

$$\mathscr{H}[\xi_u^M]+2C^{\mathscr{F}}\Delta t\sum_{n=2}^{M}\|\xi_u^n\|^2\le C\Delta t\sum_{n=2}^{M}\|\xi_u^n\|^2+C\Delta t\sum_{n=0}^{M}\left(h^{2(k+1)}+\Delta t^4+\varepsilon^2\right).$$

Using (3.2) and the discrete Gronwall inequality, we have $\|\xi_u^M\|^2\le C\left(h^{2(k+1)}+\Delta t^4+\varepsilon^2\right)$. Using triangle inequality, we obtain

$$\|u^n-u_h^n\|=\|\xi_u^n+\eta_u^n\|\le\|\xi_u^n\|+\|\eta_u^n\|\le C\left(h^{k+1}+\Delta t^2+\varepsilon\right).$$

5. Numerical Results

To verify the effectiveness of our numerical scheme, we give the numerical results based on the $L2$-1_σ formula and the $\mathscr{F}L2$-1_σ formula respectively. Now, we take $\gamma^T=(\gamma_1,\gamma_2)=(1,1)$, $\varepsilon=\frac{\Delta t^{3-\alpha}}{1000}$, the space domain $\bar{\Omega}=[0,2]\times[0,2]$ and the time interval $[0,T]=[0,1]$. The source function is

$$f(x,y,t)=\left(2t+\frac{2t^{2-\alpha}}{\Gamma(3-\alpha)}+2\pi^2t^2\right)\sin(\pi x)\sin(\pi y)+\pi t^2\left(\cos(\pi x)\sin(\pi y)+\sin(\pi x)\cos(\pi y)\right),$$

and the exact solution is $u(x,y,t)=t^2\sin(\pi x)\sin(\pi y)$.

5.1. **Tests on the CFL condition.** First, we provide the general form of the CFL condition for the convection-diffusion equation as follows $\frac{\Delta t}{h}+\frac{\Delta t}{h^2}\leq N_{CFL}$, where N_{CFL} is CFL number. Next, we will examine the impact of the CFL condition on the error stability by implementing numerical simulations. The CFL condition requires selecting an appropriate step ratio to ensure the stability and convergence of the numerical scheme. In Table 1, taking $N_{CFL}=\frac{\Delta t}{h}+\frac{\Delta t}{h^2}$, we provide the CFL numbers with different space-time step length sizes Δt and h. In Figs. 1-3, based on the CFL numbers in Table1, we plot the relationship between the error and the CFL number with different $\alpha=0.2,0.4,0.6,0.8$ in $Q^k(k=0,1,2)$ elements. In Figs. 1-3, the error curves under different parameters α have almost the same trend with changed spatial step length sizes $h=0.4,0.2,0.1$. In Fig. 1, with different spatial step length sizes $h=0.4,0.2,0.1$, the error curves exhibit similar trends for different parameters α. Specifically, for $h=0.4$, the errors tend to be stable when CFL numbers are less than 0.1367. For $h=0.2$, the errors tend to be stable when CFL numbers are less than 0.4688. For $h=0.1$, the errors tend to be stable when CFL numbers are less than 0.8594. As h decreases, the necessary CFL number needed to maintain the stable error increases. Therefore, for any spatial step length size h, it is sufficient to select Δt such that CFL numbers are less than 0.1367 in order to ensure error stability in the numerical simulation using Q^0 element. Figs. 2-3 further support this phenomenon, which exhibit a similar trend. Thus, for any spatial step size h, selecting the temporal step Δt that ensures CFL numbers are less than 2.1875 and 0.1367, we can keep the stability of error in Q^1 and Q^2 elements.

TABLE 1. The CFL number with $h=\frac{2}{N_x}$, $\Delta t=\frac{1}{M}$

h \ Δt	$\frac{1}{2}$	$\frac{1}{4}$	$\frac{1}{8}$	$\frac{1}{16}$	$\frac{1}{32}$	$\frac{1}{64}$	$\frac{1}{128}$	$\frac{1}{256}$	$\frac{1}{512}$	$\frac{1}{1024}$
0.4	4.375	2.1875	1.0938	0.5469	0.2734	0.1367	0.0684	0.0342	0.0171	0.0085
0.2	15	7.5	3.75	1.875	0.9375	0.4688	0.2344	0.1172	0.0586	0.0293
0.1	55	27.5	13.75	6.875	3.4375	1.7188	0.8594	0.4297	0.2148	0.1074

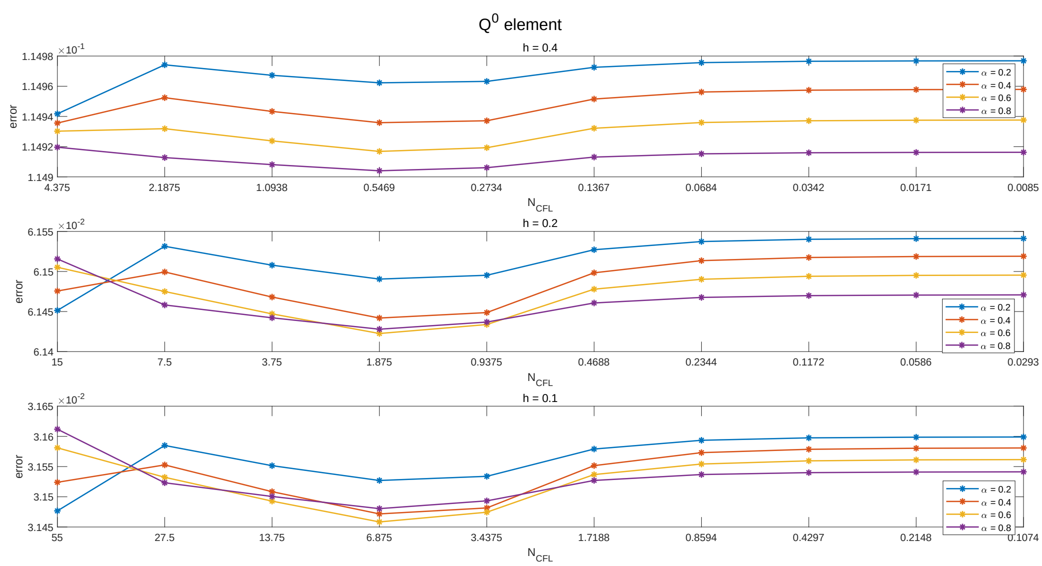

FIGURE 1. The relationship between the error and the CFL number with $\alpha=0.2,0.4,0.6,0.8$ in Q^0 element

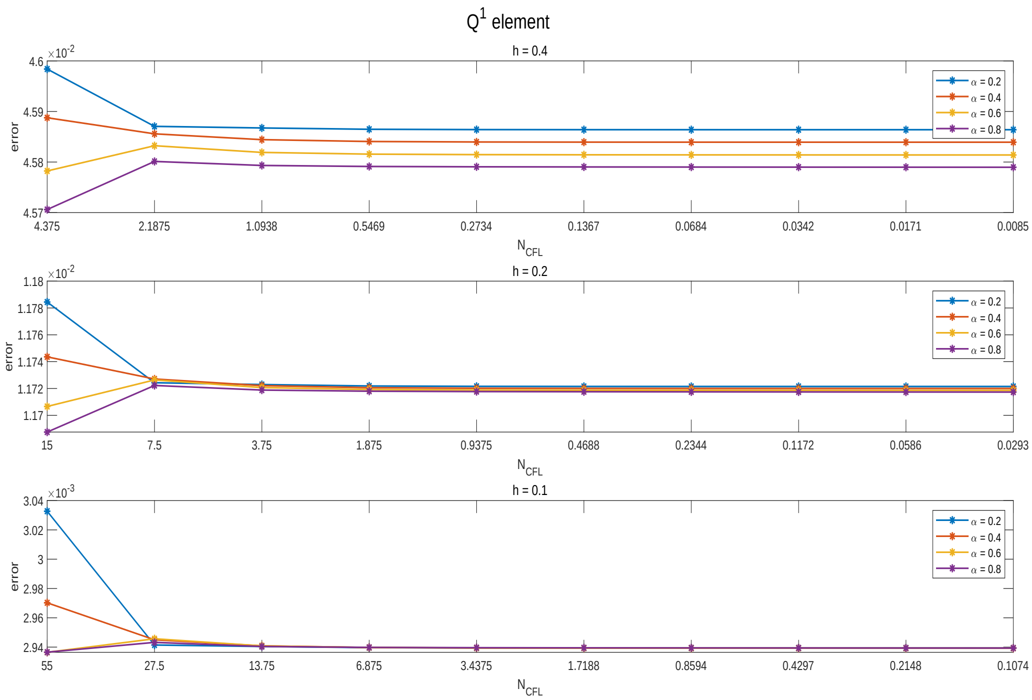

FIGURE 2. The relationship between the error and the CFL number with $\alpha = 0.2, 0.4, 0.6, 0.8$ in Q^1 element

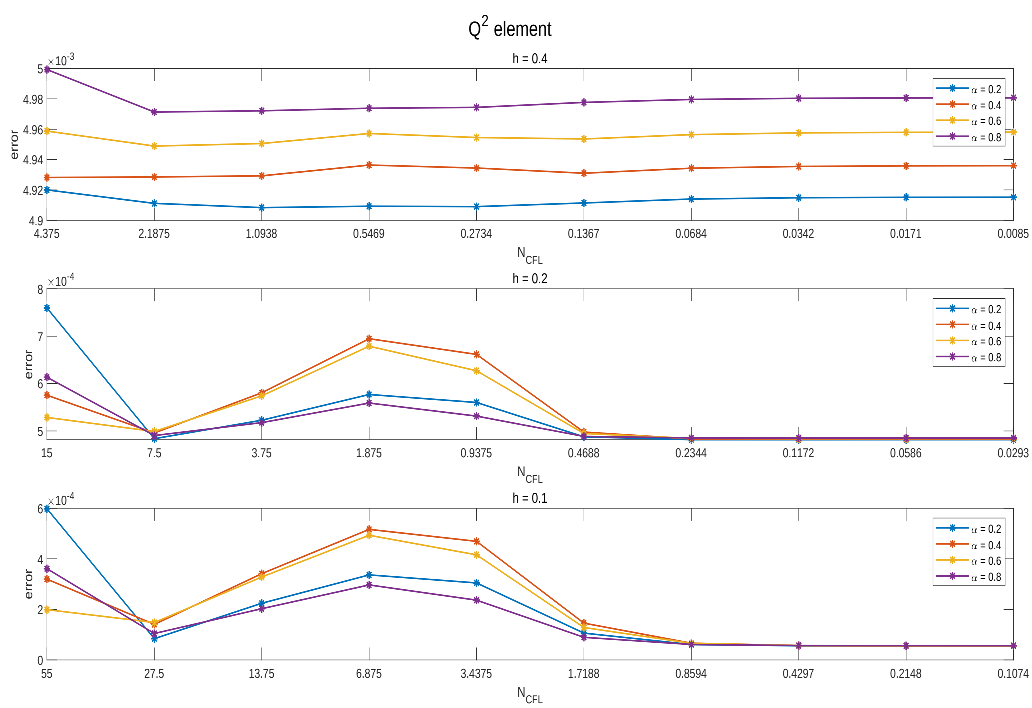

FIGURE 3. The relationship between the error and the CFL number with $\alpha = 0.2, 0.4, 0.6, 0.8$ in Q^2 element

5.2. **Convergence results.** In Table 2, to compare the accuracy of the $L2\text{-}1_\sigma$ scheme and the $\mathscr{F}L2\text{-}1_\sigma$ scheme, we show the L^2-norm error and the temporal convergence orders with different parameters α and changed space-time mesh parameters in Q^1 element. Their orders of convergence are close to 2. It is easy to verify that CFL numbers in Table 2 is $N_{CFL} = 0.875, 1.5, 2.75, 5.25$. From Fig. 2, one can be seen that CFL numbers in Table 2 are all within the stable range. In Tables 3-5, fixing the time parameter $M = 1000$ and choosing spatial mesh parameters $N = N_x \times N_y = 100, 225, 400, 625$, we get the spatial convergence accuracy with different parameters $\alpha = 0.2, 0.4, 0.6, 0.8$ in $Q^k(k = 0,1,2)$ elements for the $L2\text{-}1_\sigma$ scheme and the $\mathscr{F}L2\text{-}1_\sigma$ scheme. From Table 3, taking $k = 0$, we get the first-order spatial convergence accuracy, which is consistent with our theoretical results $O(h)$. From Table 4, taking $k = 1$, we get the second-order spatial convergence accuracy, which is consistent with our theoretical results $O(h^2)$. From Table 5, taking $k = 2$, we get the third-order spatial convergence accuracy, which is consistent with our theoretical results $O(h^3)$. The results show that the accuracy of the two schemes is the same. In Table 6, taking $\alpha = 0.5$, $N = 25$ and $M = 2000, 4000, 6000, 8000, 10000$, we present the CPU time in seconds, which shows that the $\mathscr{F}L2\text{-}1_\sigma$ scheme is more efficient than the $L2\text{-}1_\sigma$ scheme.

To observe the effect of numerical simulation more clearly, we provide some numerical solution images based on $\mathscr{F}L2\text{-}1_\sigma$ scheme. In Fig. 4, we get images of numerical solution u_h with $N = 400$, $M = 40$. In Fig. 5, we plot the error contours of $u - u_h$ with $\alpha = 0.2, 0.4, 0.6, 0.8$. In Fig. 6, we can obtain similar temporal convergence order in L^2-norm with the different fractional parameters $\alpha = 0.2, 0.4, 0.6, 0.8$. In Fig. 7, we also show the spatial convergence orders in L^2-norm based on the $Q^k(k = 0,1,2)$ elements.

TABLE 2. The temporal convergence results in L^2-norm

		$L2\text{-}1_\sigma$		$\mathscr{F}L2\text{-}1_\sigma$	
α	(N,M)	Error	Order	Error	Order
	(25,10)	4.5866E-02	–	4.5907E-02	–
0.2	(100,20)	1.1722E-02	1.9682	1.1753E-02	1.9657
	(400,40)	2.9394E-03	1.9956	2.9630E-03	1.9878
	(1600,80)	7.3535E-04	1.9990	7.4084E-04	1.9999
	(25,10)	4.5842E-02	–	4.5907E-02	–
0.4	(100,20)	1.1720E-02	1.9677	1.1770E-02	1.9636
	(400,40)	2.9393E-03	1.9955	2.9820E-03	1.9808
	(1600,80)	7.3535E-04	1.9990	7.4546E-04	2.0001
	(25,10)	4.5816E-02	–	4.5878E-02	–
0.6	(100,20)	1.1719E-02	1.9670	1.1765E-02	1.9633
	(400,40)	2.9392E-03	1.9953	2.9786E-03	1.9818
	(1600,80)	7.3535E-04	1.9989	7.4595E-04	1.9975
	(25,10)	4.5790E-02	–	4.5828E-02	–
0.8	(100,20)	1.1717E-02	1.9664	1.1743E-02	1.9644
	(400,40)	2.9391E-03	1.9952	2.9605E-03	1.9879
	(1600,80)	7.3534E-04	1.9989	7.4092E-04	1.9984

TABLE 3. The spatial convergence results in L^2-norm with $M = 1000$, $k = 0$

		$L2\text{-}1_\sigma$		$\mathscr{F}L2\text{-}1_\sigma$	
α	N	Error	Order	Error	Order
0.2	100	6.1541E-02	–	6.1541E-02	–
	225	4.1783E-02	0.9550	4.1783E-02	0.9550
	400	3.1599E-02	0.9711	3.1599E-02	0.9711
	625	2.5399E-02	0.9788	2.5399E-02	0.9788
0.4	100	6.1519E-02	–	6.1519E-02	–
	225	4.1763E-02	0.9553	4.1762E-02	0.9553
	400	3.1581E-02	0.9714	3.1581E-02	0.9714
	625	2.5383E-02	0.9790	2.5383E-02	0.9790
0.6	100	6.1496E-02	–	6.1495E-02	–
	225	4.1741E-02	0.9557	4.1741E-02	0.9557
	400	3.1562E-02	0.9717	3.1562E-02	0.9717
	625	2.5367E-02	0.9793	2.5366E-02	0.9793
0.8	100	6.1471E-02	–	6.1471E-02	–
	225	4.1718E-02	0.9560	4.1718E-02	0.9560
	400	3.1542E-02	0.9720	3.1541E-02	0.9720
	625	2.5349E-02	0.9795	2.5348E-02	0.9796

TABLE 4. The spatial convergence results in L^2-norm with $M = 1000$, $k = 1$

		$L2\text{-}1_\sigma$		$\mathscr{F}L2\text{-}1_\sigma$	
α	N	Error	Order	Error	Order
0.2	100	1.1721E-02	–	1.1722E-02	–
	225	5.2218E-03	1.9942	5.2219E-03	1.9942
	400	2.9394E-03	1.9975	2.9394E-03	1.9975
	625	1.8818E-03	1.9986	1.8818E-03	1.9985
0.4	100	1.1720E-02	–	1.1720E-02	–
	225	5.2216E-03	1.9940	5.2216E-03	1.9940
	400	2.9393E-03	1.9974	2.9393E-03	1.9974
	625	1.8818E-03	1.9985	1.8818E-03	1.9985
0.6	100	1.1718E-02	–	1.1719E-02	–
	225	5.2213E-03	1.9938	5.2214E-03	1.9938
	400	2.9392E-03	1.9974	2.9393E-03	1.9973
	625	1.8817E-03	1.9985	1.8818E-03	1.9984
0.8	100	1.1717E-02	–	1.1717E-02	–
	225	5.2210E-03	1.9937	5.2213E-03	1.9936
	400	2.9391E-03	1.9973	2.9394E-03	1.9972
	625	1.8817E-03	1.9984	1.8819E-03	1.9982

TABLE 5. The spatial convergence results in L^2-norm with $M = 1000$, $k = 2$

		$L2\text{-}1_\sigma$		$\mathscr{F}L2\text{-}1_\sigma$	
α	N	Error	Order	Error	Order
	100	4.8170E-04	–	4.8169E-04	–
	225	1.3466E-04	3.1435	1.3465E-04	3.1436
0.2	400	5.5712E-05	3.0677	5.5711E-05	3.0677
	625	2.8309E-05	3.0339	2.8313E-05	3.0333
	100	4.8280E-04	–	4.8278E-04	–
	225	1.3491E-04	3.1445	1.3490E-04	3.1445
0.4	400	5.5822E-05	3.0674	5.5825E-05	3.0671
	625	2.8401E-05	3.0283	2.8413E-05	3.0267
	100	4.8403E-04	–	4.8400E-04	–
	225	1.3524E-04	3.1448	1.3523E-04	3.1447
0.6	400	5.6013E-05	3.0640	5.6026E-05	3.0631
	625	2.8582E-05	3.0151	2.8617E-05	3.0107
	100	4.8539E-04	–	4.8531E-04	–
	225	1.3566E-04	3.1440	1.3567E-04	3.1434
0.8	400	5.6313E-05	3.0563	5.6422E-05	3.0498
	625	2.8885E-05	2.9918	2.9126E-05	2.9632

TABLE 6. CPU time in seconds with $\alpha = 0.5$, $N = 25$

	CPU time(s)	
M	$L2\text{-}1_\sigma$	$\mathscr{F}L2\text{-}1_\sigma$
2000	28.55	6.79
4000	184.55	13.37
6000	603.51	20.16
8000	1357.18	27.08
10000	2559.32	34.10

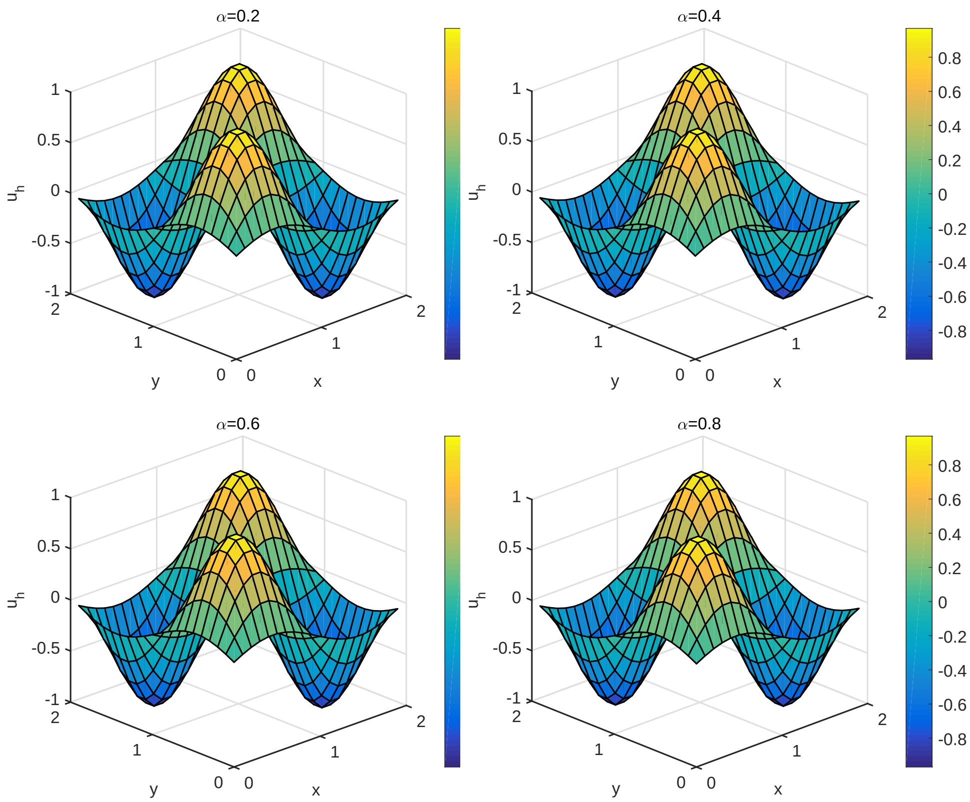

FIGURE 4. Numerical solution u_h with $N = 400$, $M = 20$

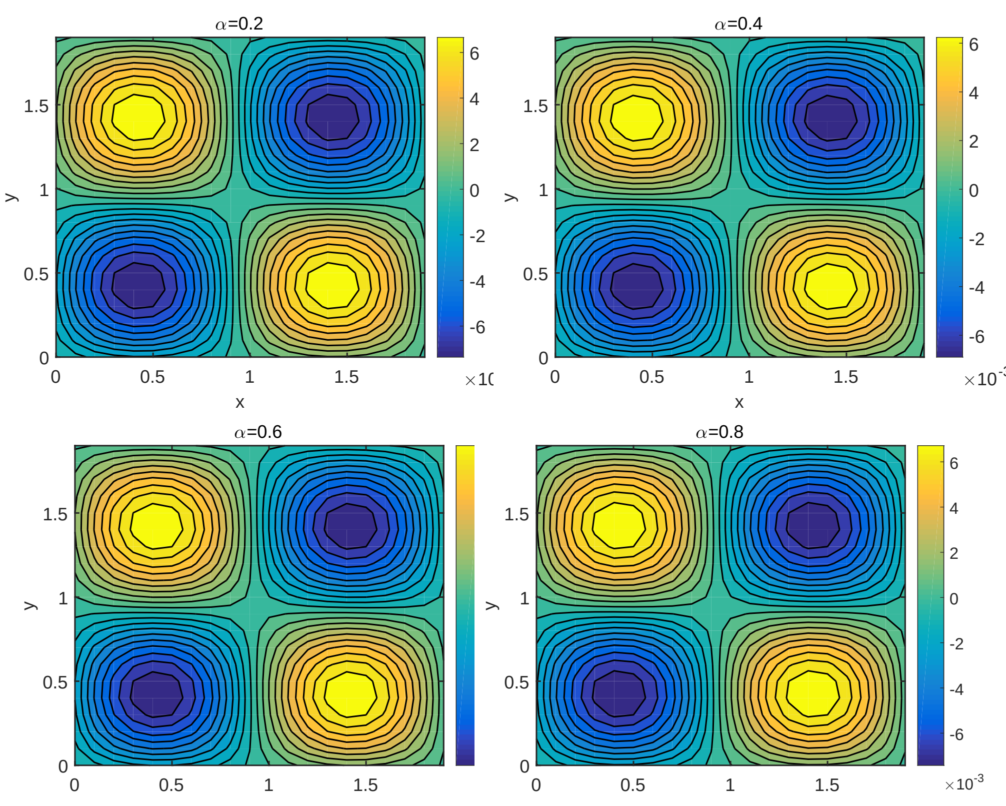

FIGURE 5. The error contours of $u - u_h$ with $\alpha = 0.2, 0.4, 0.6, 0.8$

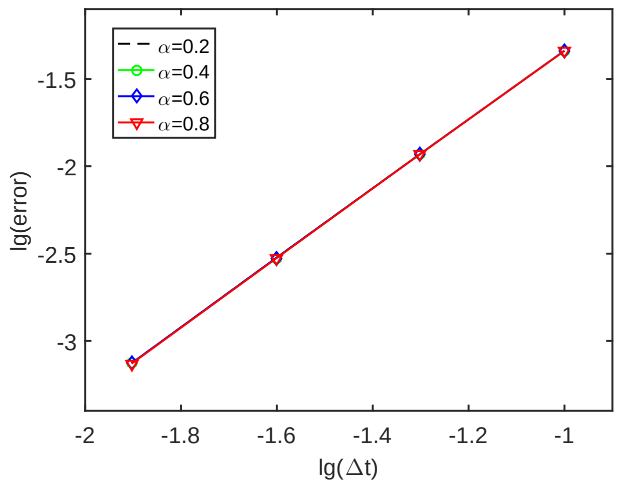

FIGURE 6. The temporal convergence orders in L^2-norm with $\alpha = 0.2, 0.4, 0.6, 0.8$

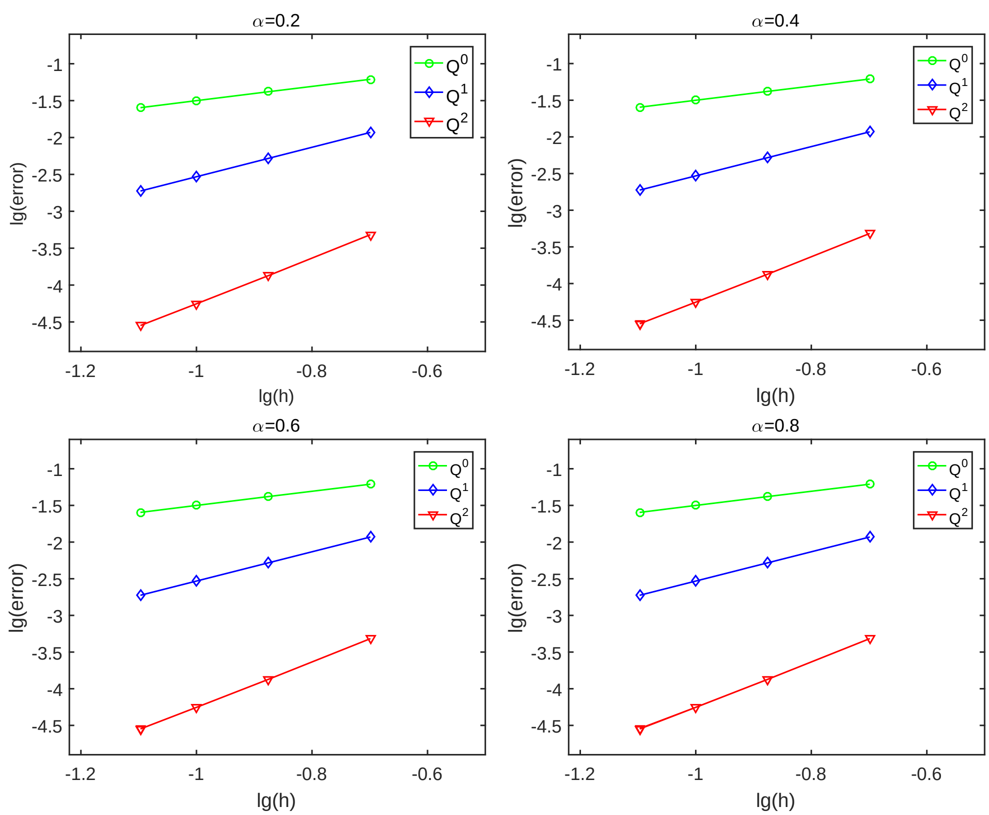

FIGURE 7. The spatial convergence orders in L^2-norm with $\alpha = 0.2, 0.4, 0.6, 0.8$

5.3. **Sensitivity of the tolerance error.** In this subsection, we verify the sensitivity of the tolerance error ε on numerical results. For this purpose, we only show the numerical performance in Q^1 element. In Table 7, fixing the temporal parameter $M = 1000$, taking spatial mesh parameters $N = N_x \times N_y = 25, 100$, and choosing different parameters $\alpha = 0.2, 0.4, 0.6, 0.8$, we obtain the error results with different parameters $\varepsilon = 10^{-2}$, 10^{-4}, 10^{-6}, $\frac{\Delta t^{3-\alpha}}{10}$, $\frac{\Delta t^{3-\alpha}}{100}$, $\frac{\Delta t^{3-\alpha}}{1000}$. Table 7 shows that changes of ε have less impact on error and convergence results. In Table 8, fixing the temporal parameter $M = 4000$ and changing the different parameters $\varepsilon = 10^{-2}$,10^{-4}, 10^{-6}, $\frac{\Delta t^{3-\alpha}}{10}$, $\frac{\Delta t^{3-\alpha}}{100}$, $\frac{\Delta t^{3-\alpha}}{1000}$, we have the number of exponentials N_{exp} and CPU time with different parameters $\alpha = 0.2, 0.4, 0.6, 0.8$. Table 8 shows that as ε decreases, both N_{exp} and CPU time increase. In Fig. 8, fixing the temporal parameter $M = 1000$ and the spatial mesh parameter $N = 1000$, we get $\mathrm{Error}_{(\varepsilon-\varepsilon_0)}$ with different parameters $\varepsilon = 10^{-2}$,10^{-4},10^{-6}, $\frac{\Delta t^{3-\alpha}}{10}$, $\frac{\Delta t^{3-\alpha}}{100}$, where $\mathrm{Error}_{(\varepsilon-\varepsilon_0)} = \mathrm{Error}_{\varepsilon} - \mathrm{Error}_{\varepsilon_0}$, $\mathrm{Error}_{\varepsilon}$ is the L^2-norm error of numerical solution u_h and exact solution u with different parameters ε. We use $\varepsilon_0 = \frac{\Delta t^{3-\alpha}}{1000}$ as a reference standard to test the difference between $\mathrm{Error}_{\varepsilon}$ and $\mathrm{Error}_{\varepsilon_0}$. Fig. 8 clearly illustrates that decreasing ε leads to a decrease of error. In summary, the choice of ε should balance accuracy and computational cost. Furthermore, one can be seen from the convergence results in Table 7 that the sensitivity of ε on numerical results is not significant.

TABLE 7. $\mathrm{Error}_{\varepsilon}$ with $M = 1000$

α	N \ ε	10^{-2}	10^{-4}	10^{-6}	$\frac{\Delta t^{3-\alpha}}{10}$	$\frac{\Delta t^{3-\alpha}}{100}$	$\frac{\Delta t^{3-\alpha}}{100}$
0.2	5	4.5880E-02	4.58641E-02	4.58639E-02	4.58639E-02	4.58639E-02	4.58639E-02
	10	1.1728E-02	1.17216E-02	1.17215E-02	1.17215E-02	1.17215E-02	1.17215E-02
	Order	1.9679	1.9682	1.9682	1.9682	1.9682	1.9682
0.4	5	4.5847E-02	4.58393E-02	4.58392E-02	4.58392E-02	4.58392E-02	4.58392E-02
	10	1.1723E-02	1.17201E-02	1.17200E-02	1.17200E-02	1.17200E-02	1.17200E-02
	Order	1.9674	1.9676	1.9676	1.9676	1.9676	1.9676
0.6	5	4.5819E-02	4.58140E-02	4.58140E-02	4.58140E-02	4.58140E-02	4.58140E-02
	10	1.1721E-02	1.17186E-02	1.17185E-02	1.17185E-02	1.17185E-02	1.17185E-02
	Order	1.9669	1.9670	1.9670	1.9670	1.9670	1.9670
0.8	5	4.5792E-02	4.57897E-02	4.57897E-02	4.57897E-02	4.57897E-02	4.57897E-02
	10	1.1718E-02	1.17173E-02	1.17173E-02	1.17173E-02	1.17173E-02	1.17173E-02
	Order	1.9663	1.9664	1.9664	1.9664	1.9664	1.9664

TABLE 8. N_{exp} and CPU time in seconds with $M = 4000$, $N = 100$

	ε	10^{-2}	10^{-4}	10^{-6}	$\frac{\Delta t^{3-\alpha}}{10}$	$\frac{\Delta t^{3-\alpha}}{100}$	$\frac{\Delta t^{3-\alpha}}{100}$
$\alpha = 0.2$	N_{exp}	16	25	35	59	64	69
	CPU time(s)	50.71	59.12	65.06	84.99	88.86	91.80
$\alpha = 0.4$	N_{exp}	16	25	35	56	61	66
	CPU time(s)	53.02	59.67	67.27	82.44	87.86	90.30
$\alpha = 0.6$	N_{exp}	16	25	35	52	57	63
	CPU time(s)	57.57	59.86	65.71	78.50	81.73	88.32
$\alpha = 0.8$	N_{exp}	16	26	35	49	54	59
	CPU time(s)	50.58	60.36	70.71	81.41	88.05	92.12

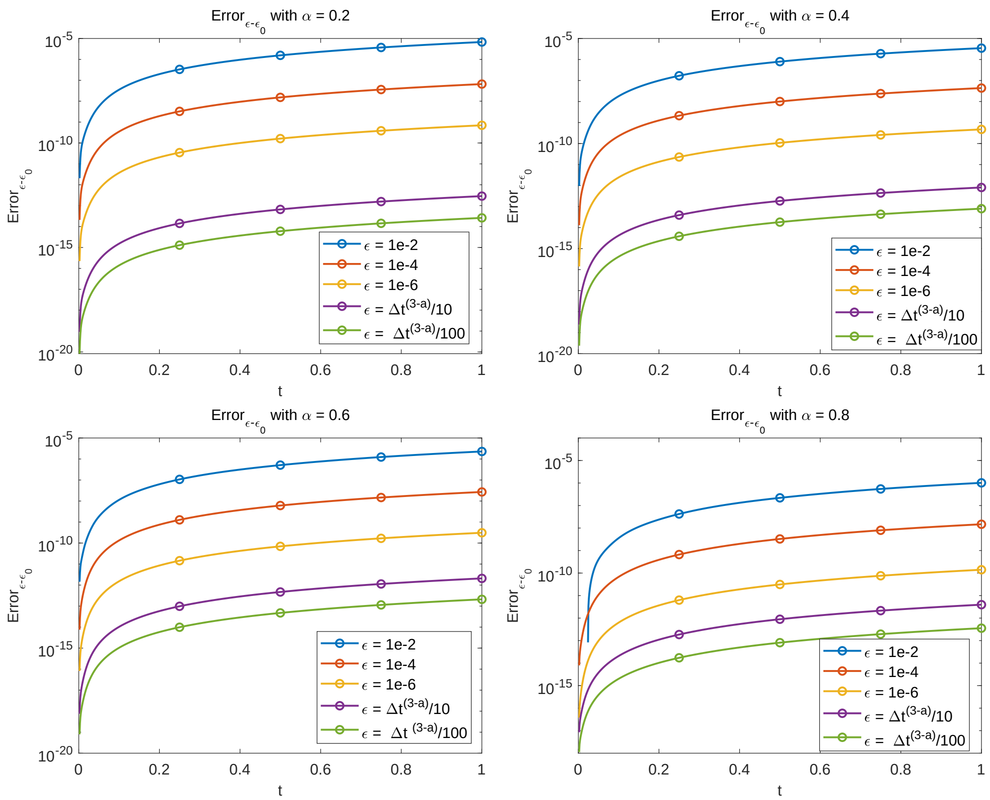

FIGURE 8. Error$_{(\varepsilon-\varepsilon_0)}$ with $\alpha = 0.2, 0.4, 0.6, 0.8$

6. CONCLUDING REMARKS

In this article, the spatial LDG method with the second-order time approximation scheme combined with the $\mathscr{F}L2\text{-}1_\sigma$ formula for the two-dimensional fractional mobile / immobile convection-diffusion model was presented. The detailed proofs of stability and errors $O(\Delta t^2 + h^{k+1} + \varepsilon)$ in L^2-norm were presented. The validity and feasibility of the algorithm in solving the two-dimensional time-fractional convection-diffusion model were illustrated by the numerical results calculated by the LDG method. Specifically, the CFL condition was provided and the relationship between the CFL number and the error in numerical simulations was analyzed. In addition, the comparison of CPU time between the $\mathscr{F}L2\text{-}1_\sigma$ scheme and the $L2\text{-}1_\sigma$ scheme confirmed that the $\mathscr{F}L2\text{-}1_\sigma$ scheme was more efficient. Finally, by changing the parameter ε for the $\mathscr{F}L2\text{-}1_\sigma$ scheme, the sensitivity of ε on numerical results was analyzed.

Acknowledgments
The authors thank the reviewers and the editor very much for their valuable comments and suggestions for improving our work. This work was supported by the National Natural Science Foundation of China (12061053, 12161063, and 12120101001), Australian Research Council via the Discovery Projects (DP 180103858 and DP 190101889), Natural Science Foundation of Inner Mongolia (2022LHMS01004), Young Innovative Talents Project of Grassland Talents Project and Program for Innovative Research Team in Universities of Inner Mongolia Autonomous Region (NMGIRT2413 and NMGIRT2207).

REFERENCES

[1] R. Schumer, D.A. Benson, M.M. Meerschaert, B. Baeumer, Fractal mobile/immobile solute transport, Water Resour. Res. 39(10) (2003), 1296-1307.

[2] H. Zhang, F. Liu, M.S. Phanikumar, M.M. Meerschaert, A novel numerical method for the time variable fractional order mobile-immobile advection-dispersion model, Comput. Math. Appl. 66(5) (2013), 693-701.

[3] H. Liu, X.C. Zheng, C.J. Chen, H. Wang, A characteristic finite element method for the time-fractional mobile/immobile advection diffusion model, Adv. Comput. Math. 47 (2021), 1-19.

[4] B. Yu, X.Y. Jiang, H.T. Qi, Numerical method for the estimation of the fractional parameters in the fractional mobile/immobile advection-diffusion model, Int. J. Comput. Math. 95 (2018), 1131-1150.

[5] J.F. Wang, T.Q. Liu, H. Li, Y. Liu, S. He, Second-order approximation scheme combined with H^1-Galerkin MFE method for nonlinear time fractional convection-diffusion equation, Comput. Math. Appl. 73 (2017), 1182-1196.

[6] C.J. Chen, H. Liu, X.C. Zheng, H. Wang, A two-grid MMOC finite element method for nonlinear variable-order time-fractional mobile/immobile advection-diffusion equations, Comput. Math. Appl. 79 (2020), 2771-2783.

[7] H. Zhang, X.Y. Jiang, F.W. Liu, Error analysis of nonlinear time fractional mobile/immobile advection-diffusion equation with weakly singular solutions, Fract. Calc. Appl. Anal. 24 (2021), 202-224.

[8] B. Cockburn, C.W. Shu, The local discontinuous Galerkin method for time-dependent convection-diffffusion systems, SIAM J. Numer. Anal. 35 (1998), 2440-2463.

[9] Y. Liu, M. Zhang, H. Li, J.C. Li, High-order local discontinuous Galerkin method combined with WSGD-approximation for a fractional subdiffusion equation, Comput. Math. Appl. 73 (2017), 1298-1314.

[10] C.P. Li, Z. Wang, The local discontinuous Galerkin finite element methods for Caputo-type partial differential equations: Numerical analysis, Appl. Numer. Math. 140 (2019), 1-22.

[11] M. Zhang, Y. Liu, H. Li, High-order local discontinuous Galerkin algorithm with time second-order schemes for the two-dimensional nonlinear fractional diffusion equation, Commun. Appl. Math. Comput. 2 (2020), 613-640.

[12] Y.X. Niu, J.F. Wang, Y. Liu, H. Li, Z.C. Fang, Local discontinuous Galerkin method based on a family of second-order time approximation schemes for fractional mobile/immobile convection-diffusion equations, Appl. Numer. Math. 179 (2022), 149-169.

[13] Y.W. Du, Y. Liu, H. Li, Z.C. Fang, S. He, Local discontinuous Galerkin method for a nonlinear time-fractional fourth-order partial differential equation, J. Comput. Phys. 344 (2017), 108-126.

[14] C. Li, S.M. Liu, Local discontinuous Galerkin method for a nonlocal viscous conservation laws, Int. J. Numer. Meth. Fluids 93 (2021), 197-219.

[15] C. Li, X.R. Sun, F.Q. Zhao, LDG schemes with second order implicit time discretization for a fractional sub-diffusion equation, Results Appl. Math. 4 (2019), 100079.

[16] M. Zhang, Y. Liu, H. Li, High-order local discontinuous Galerkin method for a fractal mobile/immobile transport equation with the Caputo-Fabrizio fractional derivative, Numer. Meth. Part. Differ. Equ. 35 (2019), 1588-1612.

[17] C.P. Li, D.X. Li, Z. Wang, L1/LDG method for the generalized time-fractional Burgers equation, Math. Comput. Simul. 187 (2021), 357-378.

[18] W.P. Yuan, Y.P. Chen, Y.Q. Huang, A local discontinuous Galerkin method for time-fractional Burgers equations, East Asian J. Appl. Math. 10 (2020), 818-837.

[19] M.H. Song, J.F. Wang, Y. Liu, H. Li, Local discontinuous Galerkin method combined with the $L2$ formula for the time fractional Cable model, J. Appl. Math. Comput. 68 (2022), 4457-4478.

[20] J. Eshaghi, S. Kazem, H. Adibi, The local discontinuous Galerkin method for 2D nonlinear time-fractional advection-diffusion equations, Eng. Comput. 35 (2019), 1317-1332.

[21] W.H. Deng, J.S. Hesthaven, Local discontinuous Galerkin methods for fractional ordinary differential equations, BIT Numer. Math. 55 (2015), 967-985.

[22] W.P. Yuan, Y.P. Chen, Y.Q. Huang, A local discontinuous Galerkin method for time-fractional Burgers equations, East Asian J. Appl. Math. 10 (2020), 818-837.

[23] L.L. Wei, Analysis of a new finite difference/local discontinuous Galerkin method for the fractional diffusion-wave equation, Appl. Math. Comput. 304 (2017), 180-189.
[24] A.A. Alikhanov, A new difference scheme for the time fractional diffusion equation, J. Comput. Phys. 280 (2015), 424-438.
[25] H. Sun, Z.Z. Sun, G.H. Gao, Some temporal second order difference schemes for fractional wave equations, Numer. Meth. Part. Differ. Equ. 32 (2016), 970-1001.
[26] C.B. Huang, N. An, X.J. Yu, A local discontinuous Galerkin method for time-fractional diffusion equation with discontinuous coefficient, Appl. Numer. Math. 151 (2020), 367-379.
[27] Z. Wang, L.H. Sun, J.X. Cao, Local discontinuous Galerkin method coupled with nonuniform time discretizations for solving the time-fractional Allen-Cahn equation, Fractal Fract. 6 (2022), 349.
[28] S.D. Jiang, J.W. Zhang, Q. Zhang, Z.M. Zhang, Fast evaluation of the Caputo fractional derivative and its applications to fractional diffusion equations, Commun. Comput. Phys. 21 (2017), 650-678.
[29] Y.G. Yan, Z.Z. Sun, J.W. Zhang, Fast evaluation of the Caputo fractional derivative and its applications to fractional diffusion equations: a second-order scheme, Commun. Comput. Phys. 22 (2017), 1028-1048.
[30] Y.X. Liang, Z.S. Yao, Z.B. Wang, Fast high order difference schemes for the time fractional telegraph equation, Numer. Meth. Part. Differ. Equ. 36 (2020), 154-172.
[31] B. Alpert, L. Greengard, T. Hagstrom, Rapid evaluation of nonreflecting boundary kernels for time-domain wave propagation, SIAM J. Numer. Anal. 37 (2000), 1138-1164.
[32] L. Greengard, P. Lin, Spectral approximation of the free-space heat kernel, Appl. Comput. Harmon. Anal. 9 (2000), 83-97.
[33] G. Beylkin, L. Monzón, Approximation by exponential sums revisited, Appl. Comput. Harmon. Anal. 28 (2010), 131-149.
[34] S.L. Lei, H.W. Sun, A circulant preconditioner for fractional diffusion equations, J. Comput. Phys. 242 (2013) 715-725.
[35] B. Cockburn, G. Kanschat, I. Perugia, D. Schötzau, Superconvergence of the local discontinuous Galerkin method for elliptic problems on Cartesian grids, SIAM J. Numer. Anal. 39 (2001), 264-285.